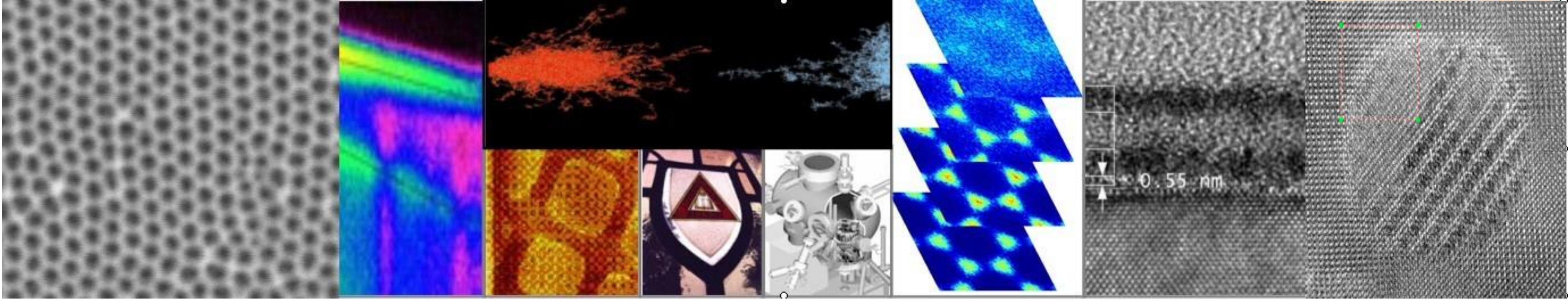

Ion Beam Analysis and Modification for Current Issues in Surface Science

Lyudmila V. Goncharova
Department of Physics and Astronomy,
Western University, London, Ontario
lgonchar@uwo.ca

Western

Outline

- Production of Ion Beams
- Basics of Ion-Solid Interactions

I: Ion Beam Analyses

- Rutherford Backscattering Spectrometry
- Elastic Recoil Detection
- Medium Energy Ion Scattering
- Research Examples: interfacial analysis of complex oxide thin film stacks; diffusion and oxidation processes with sub-nm resolution

II: Ion Beam Modification

- Implantation
- Research Examples: formation of Si and Ge quantum dots

- Conclusions
- References

Tandetron Ion Scattering facility at UWO

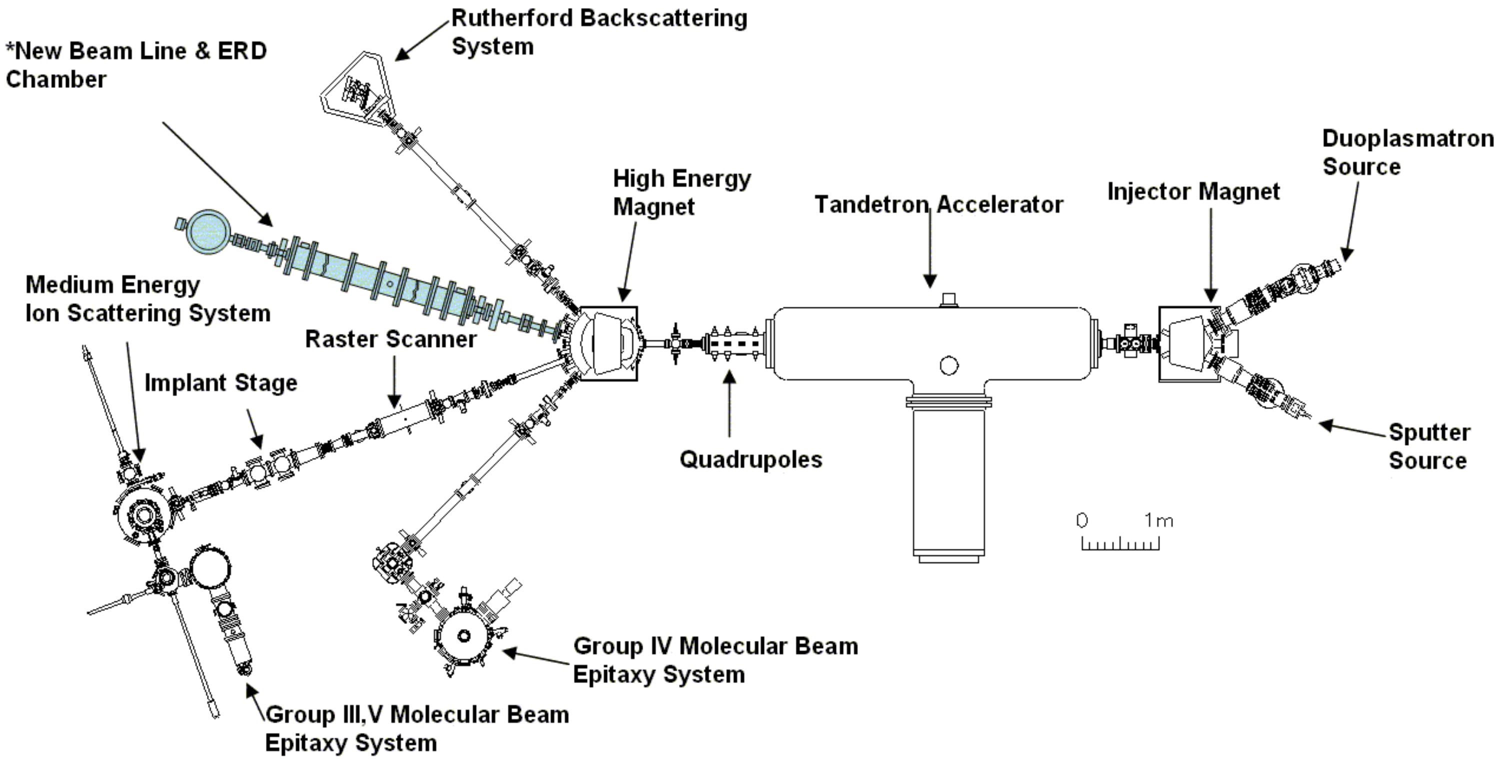

Rutherford Backscattering (RBS) and Medium Energy Ion Scattering (MEIS)
Elastic Recoil Detection (ERD)
Nuclear Reaction Analysis (NRA)
Particle-Induced X-ray Emission (PIXE)
Various implantation capabilities…

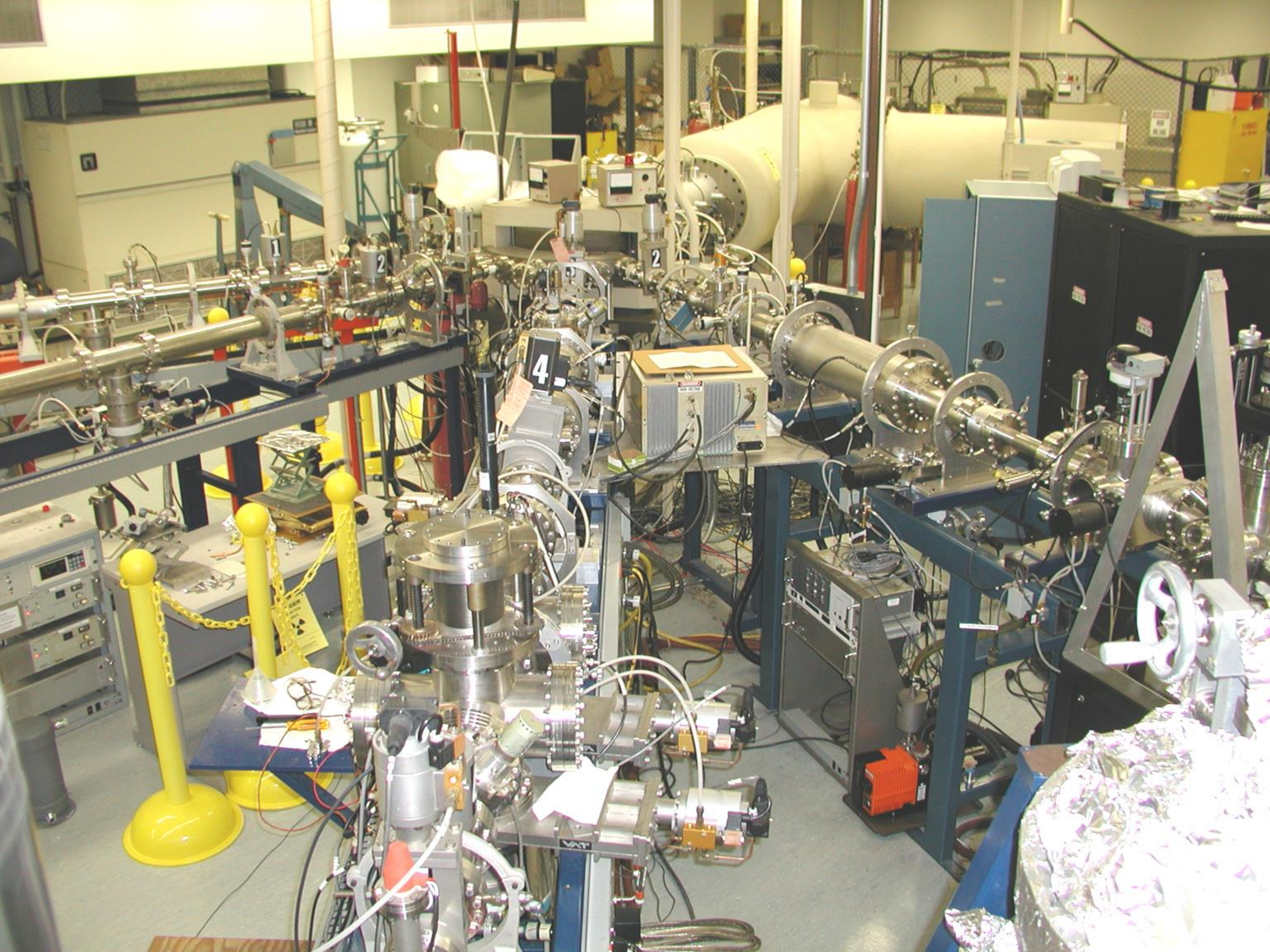
1
2
2
4

Tandetron operating principle

(1) Begin with negative ions via sputtering for most species

(2) Accelerate to kinetic energy = qV_t where V_t = terminal voltage (MV) and q_i = -1 so that $E_t \equiv V_t$ [MeV]

(3) Ions traverse a stripper gas at the high voltage terminal to produce a charge state distribution of positive ions

(4) Accel/decel mode is available when the stripper gas is ***OFF***: used for $E_{ion} \leq 100$ keV and the incident ions then have q_i = -1

Inside Tandetron…

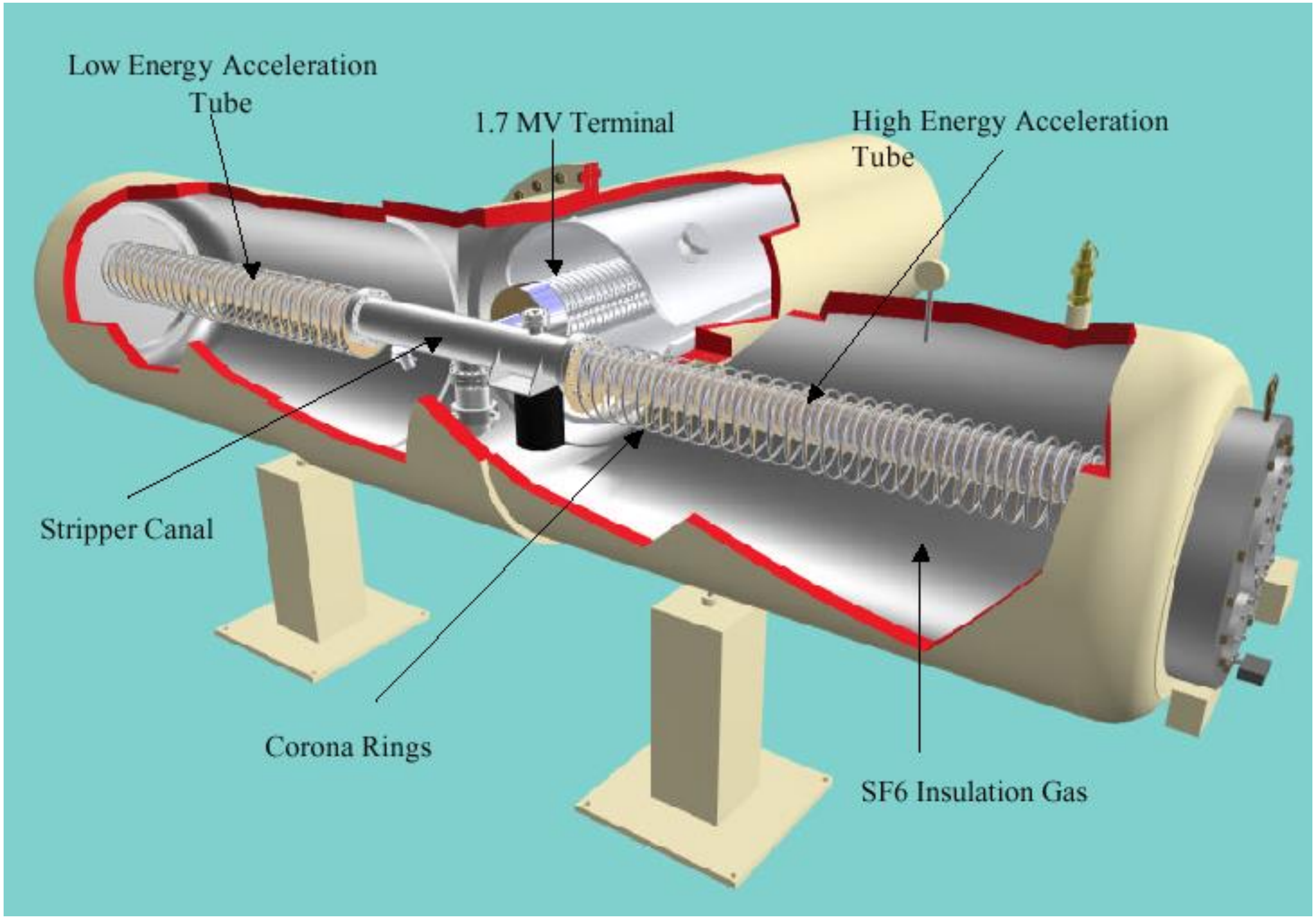

Ion Beam Analysis

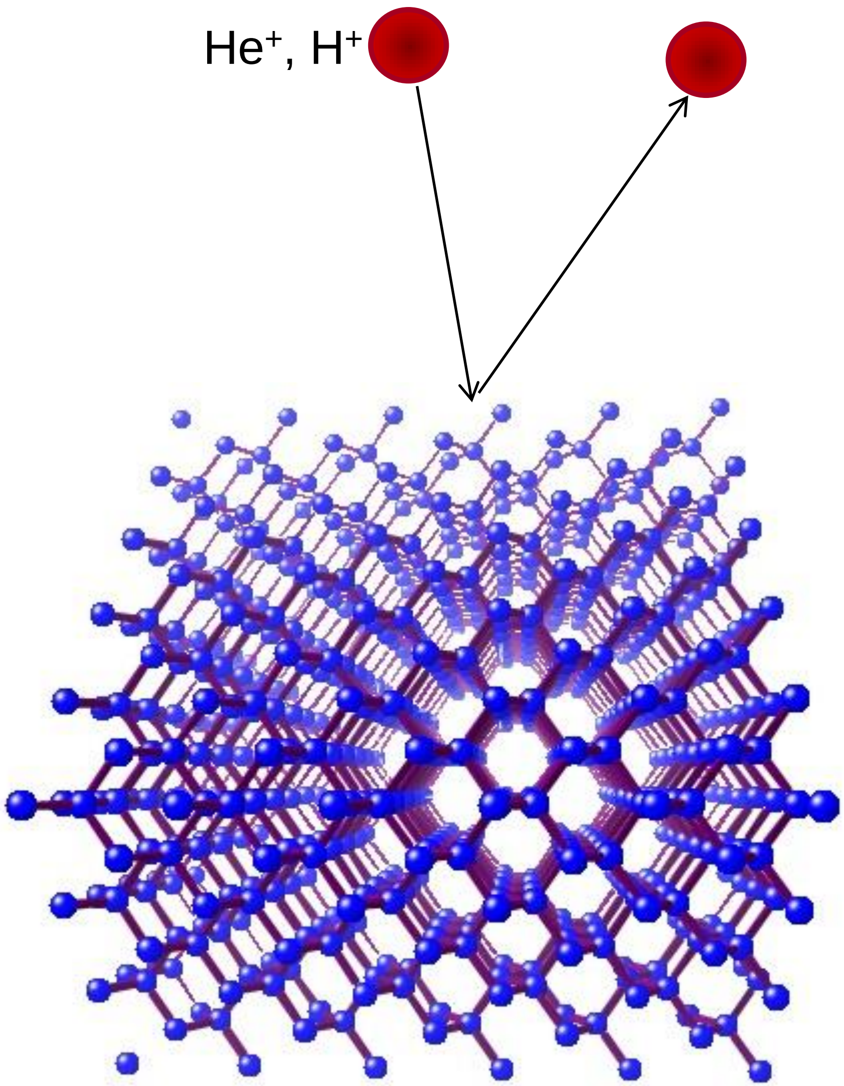

(1) elastic scattering
⇒ Rutherford Backscattering

(2) fast recoils arising from elastic scattering
⇒ Elastic Recoil Detection

(3) steering effects due to the crystalline structure of target atoms (channeling)

(4) inelastic processes: energy loss as a function of depth

(5) X-ray emission (PIXE) and nuclear reactions (NRA)

Rutherford Backscattering Spectrometry

Elastic Collisions!

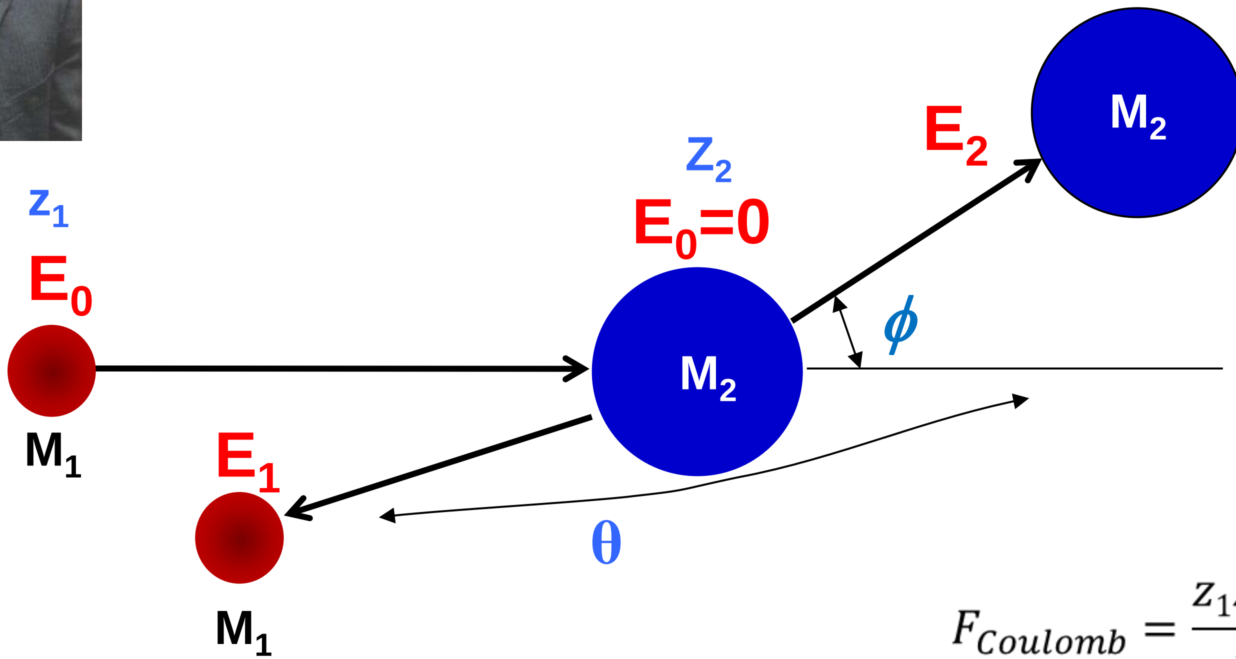

$$F_{Coulomb} = \frac{z_1 Z_2 e^2}{r^2}$$

$$\frac{1}{2} M_1 v^2 = \frac{1}{2} M_1 v_1^2 + \frac{1}{2} M_2 v_2^2 \qquad \text{(Eq.1)}$$

$$M_1 v = M_1 v_1 \cos\theta + M_2 v_2 \cos\phi \qquad \text{(Eq.2)}$$

$$0 = M_1 v_1 \sin\theta - M_2 v_2 \sin\phi \qquad \text{(Eq.3)}$$

$$E_1 = E_0 \left[\frac{\left(M_2^2 - M_1^2 \sin^2\theta\right)^{1/2} + M_1 \cos\theta}{M_2 + M_1} \right]^2$$

Charged Particle Detectors

Schematic diagram of the operation of a surface barrier detector (SBD)

- Silicon disc with gold film mounted in the detector housing
-
- He++ particle is forming holes and electrons over its penetration path.
- The energy band diagram of a reverse biased detector (positive polarity on n-type silicon) shows the electrons and holes swept apart by the high electric field within the depletion region.

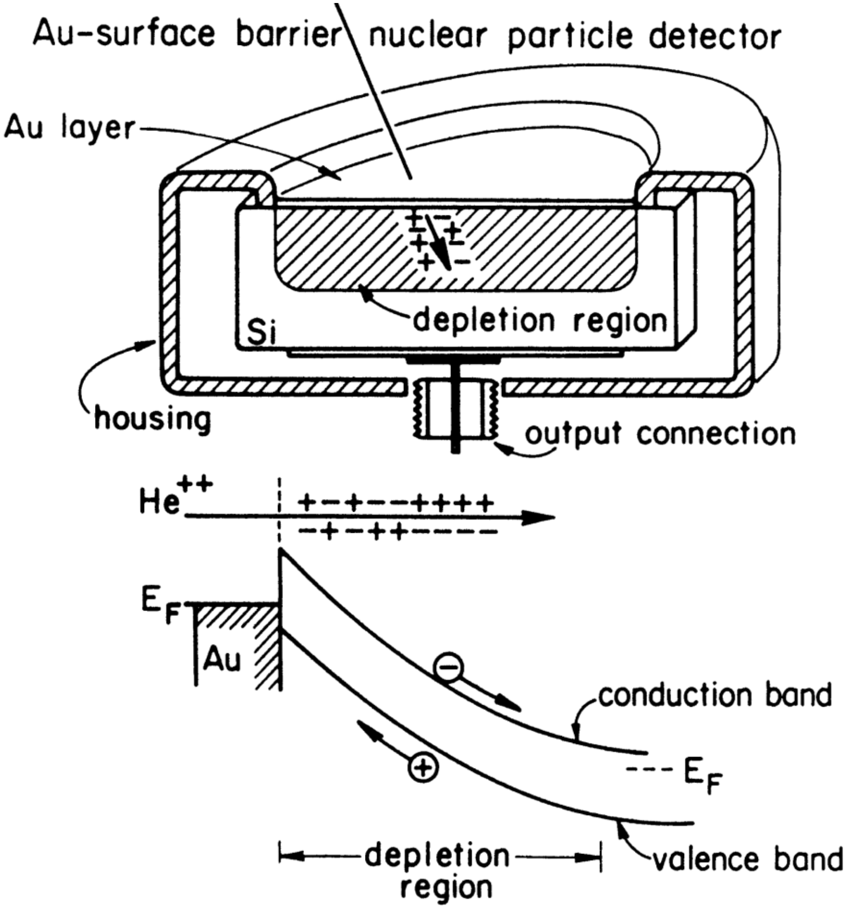

Scattering kinematics: example 1

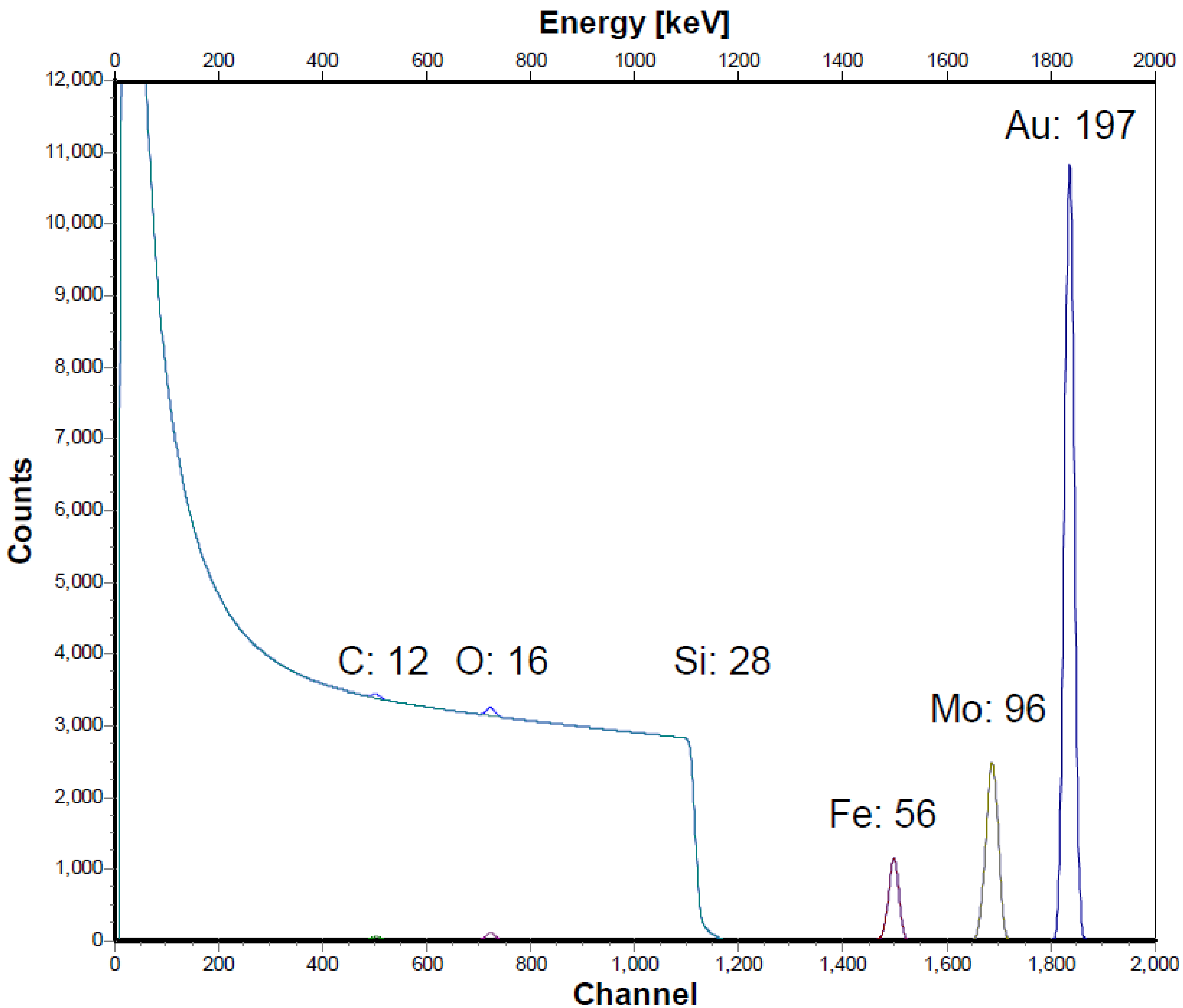

2MeV $^{4}He^{+}$, θ=165^{o}

Backscattered from

C, O, Fe, Mo, Au

3×10^{16} atoms/cm^{2} each

on Si substrate

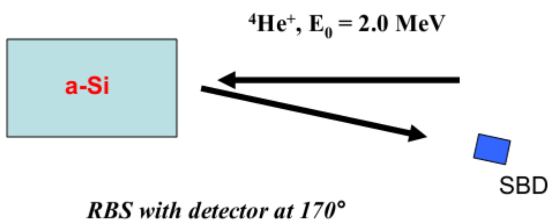

Key features of RBS

Ability to quantify depth profile of buried species with a precision of ~ 3%

Qualitative information: **kinematic factor,** k

$$k = \frac{E_1}{E_o} = \left[\frac{\left(M_2^2 - M_1^2 \sin^2\theta\right)^{1/2} + M_1 \cos\theta}{M_2 + M_1} \right]^2$$

Quantitative: **scattering cross section**, σ

$$\frac{d\sigma}{d\Omega} \equiv \sigma(\theta) = \left(\frac{Z_1 Z_2 e^2}{4E \sin^2\left(\frac{\theta}{2}\right)} \right)^2$$

Scattering kinematics: example 2

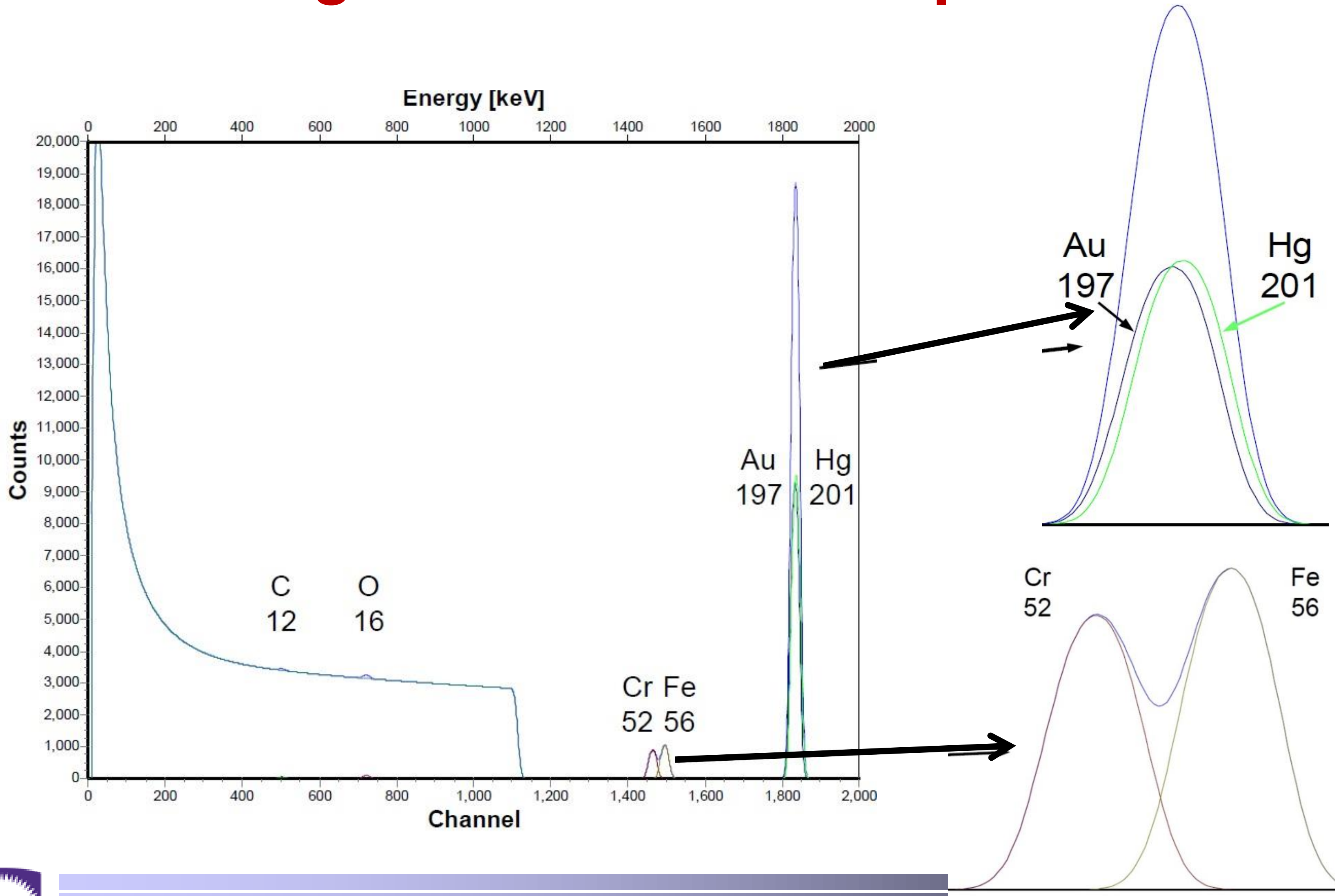

⇒ **Decreased mass resolution for heavier elements**

Rutherford Cross Section

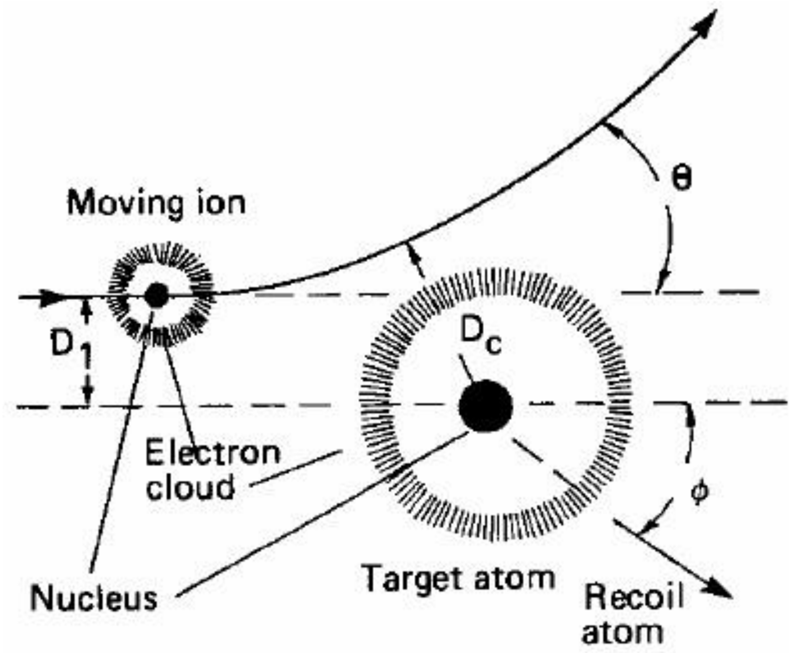

- Neglecting shielding by electron clouds
- Distance of closest approach large enough that nuclear force is negligible

⇒ Rutherford scattering cross section

$$\frac{d\sigma}{d\Omega} \equiv \sigma(\theta) = \left(\frac{Z_1 Z_2 e^2}{4E \sin^2\left(\frac{\theta}{2}\right)} \right)^2$$

Note that sensitivity increases with:

- Increasing Z_1
- Increasing Z_2
- Decreasing E

RBS spectra from thin and thick films

The integrated peak count A_i for each element on the surface can be calculated using this equation:

$$A_i = (Nt)_i \times Q \times \Omega \times \frac{\sigma(E,\theta)}{cos\theta}$$

where
$(Nt)_i$ is areal density, atoms per unit area;
Q – ion beam fluency;
Ω – solid angle of the detector;
$\sigma(E, \theta)/cos\,\theta$ – cross section of an element

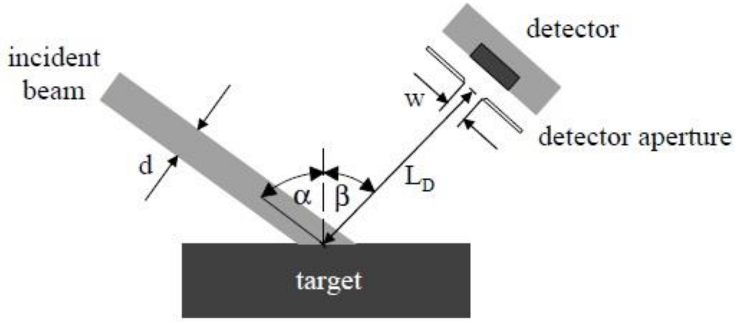

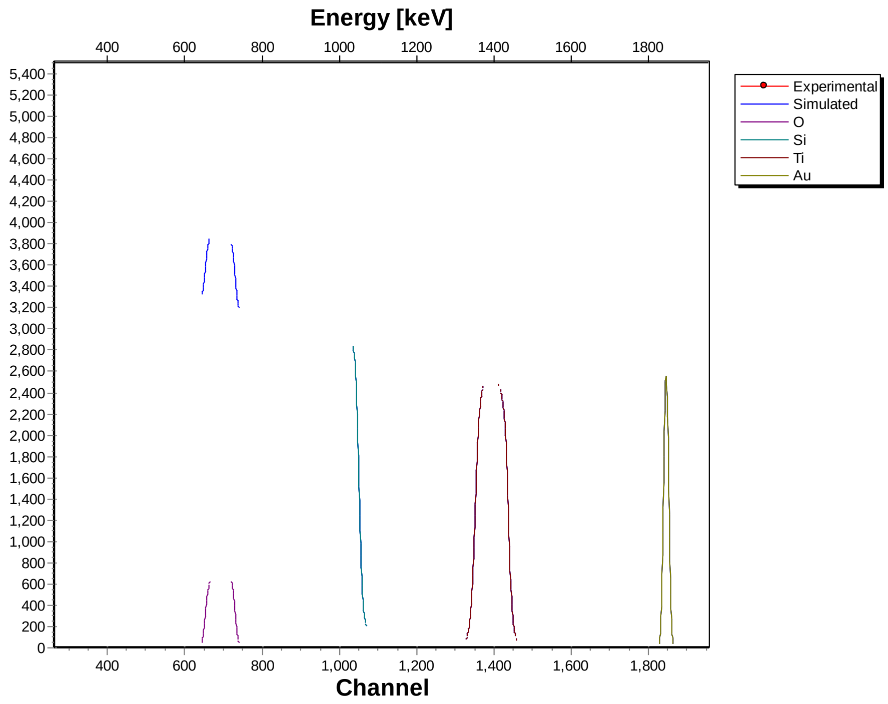

Ion dose (fluency), solid angle, cross section

- **Ion dose (fluency), the number of incident particles (collected charge)**
  - measured by Faradey cup
  - $Q = I \times t$

- **Solid angle, in steradians, sr**
  - stays constant for a particular detector/detector slit
  - need to be verified by the calibration standard measurements

- **Cross section (or differential cross section), in cm^2/sr of the element**
  - well known (tabulated) in Rutherford cross section regime

Areal density: note about units

Areal density = $\rho\, t$ [g/cm^2],

where ρ = g/cm^3, t = cm

$$\longrightarrow \quad \frac{N_0\, \rho\, t}{M} \quad [\text{at./cm}^2]$$

where M = atomic mass [amu], N_0 = Avogadro's number

In absolute numbers – close to thickness in Å

Thickness measurement

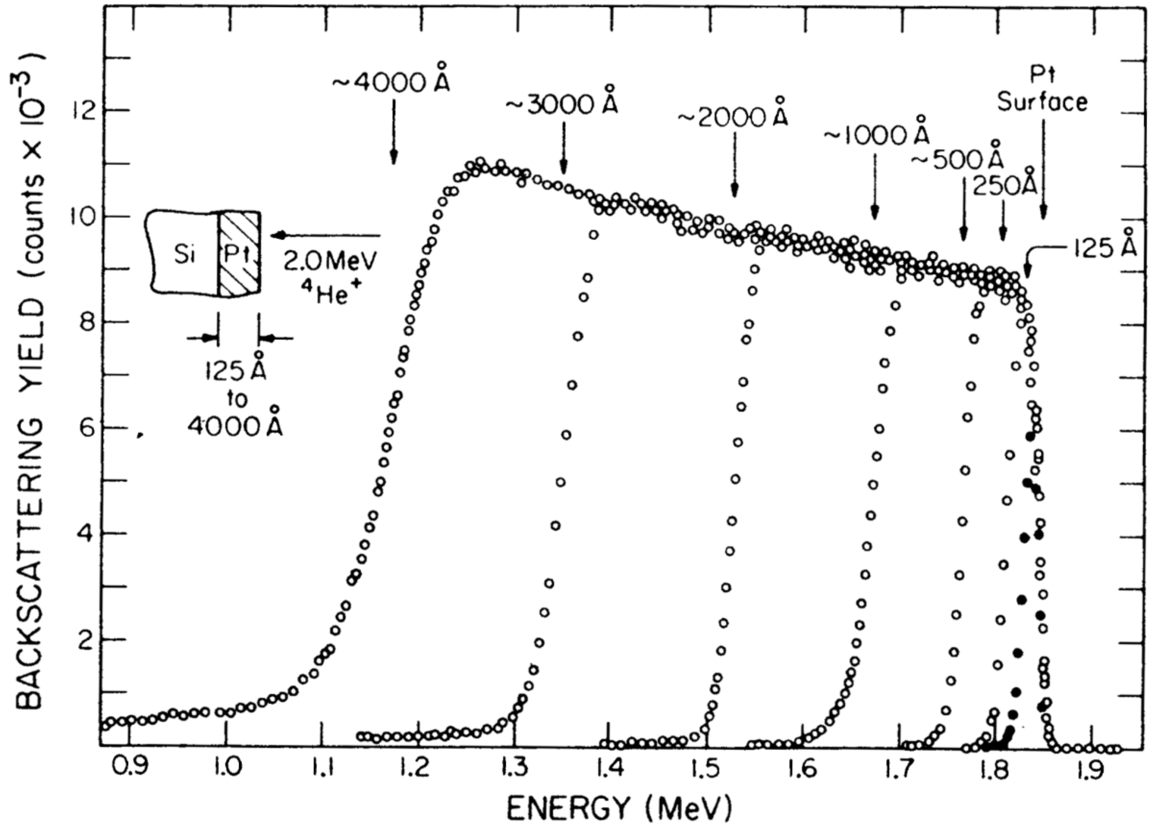

RBS Spectrum of a thick film

- Target is divided into thin sublayers ("slabs")
- Calculate backscattering from front and back side of each sublayer taking energy loss into account
- For each isotope of each element in sublayer

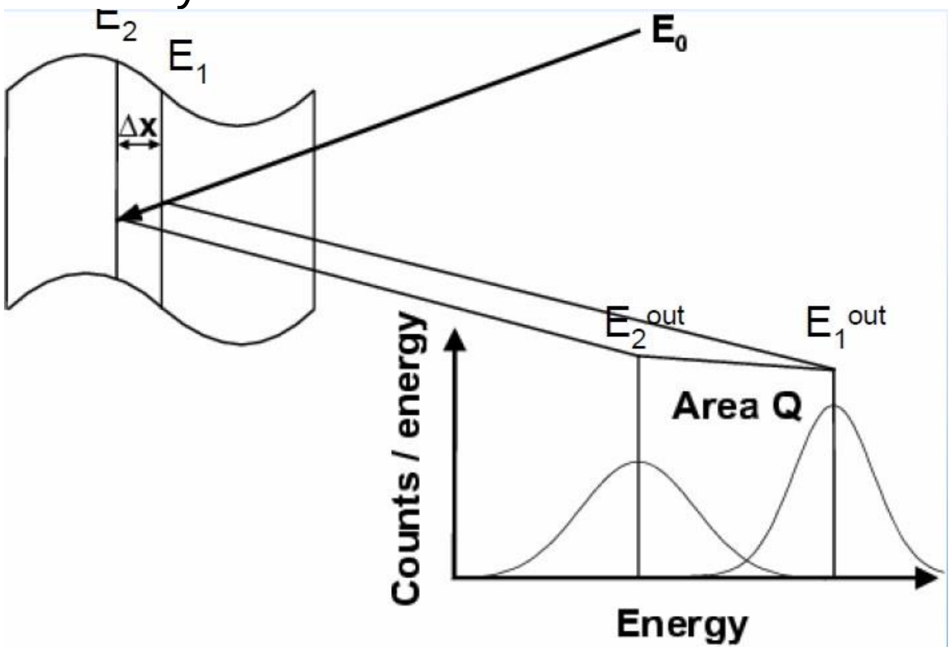

Stoichiometry

2MeV $^4He^+$, backscattered from ceramic films on Si substrate

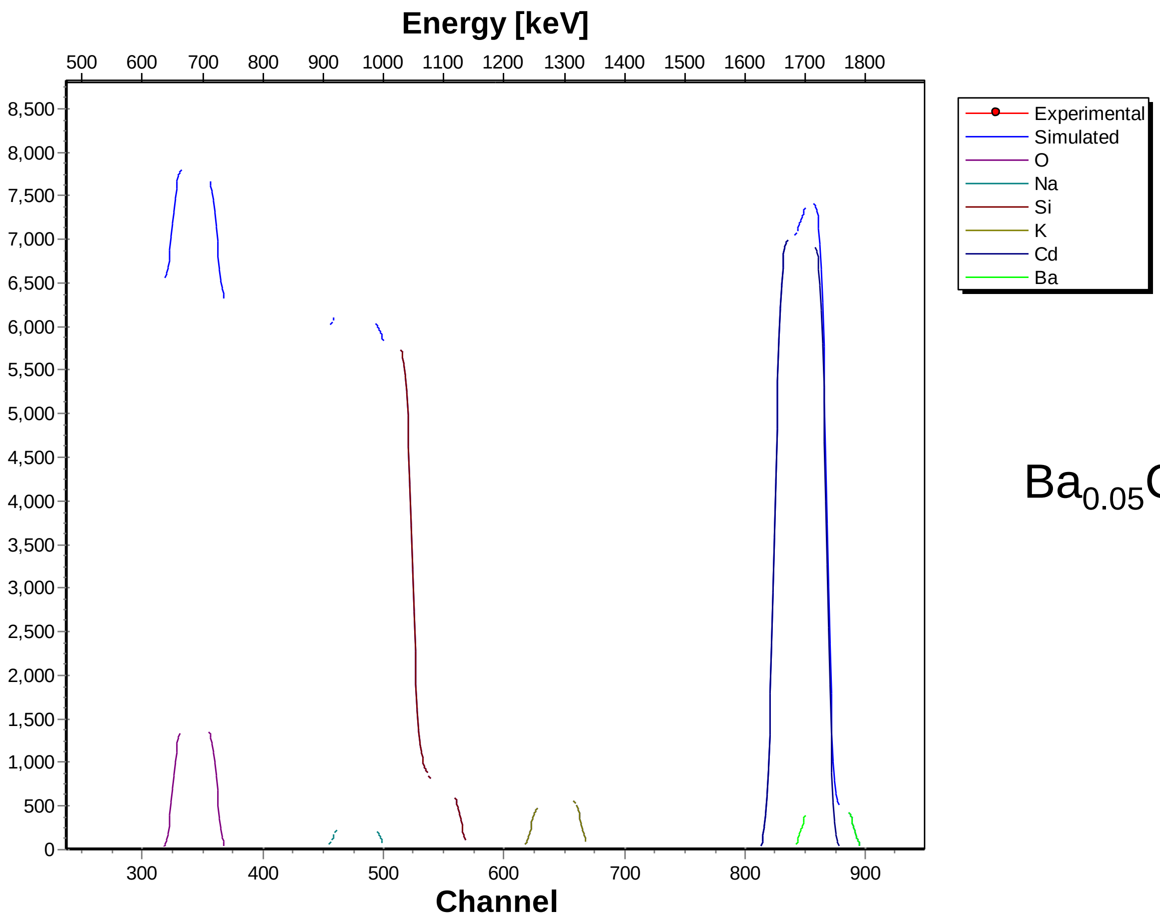

$Ba_{0.05}Cd_2KSi_2NaO_4/Si$

Ion channeling and blocking

Si (diamond structure)

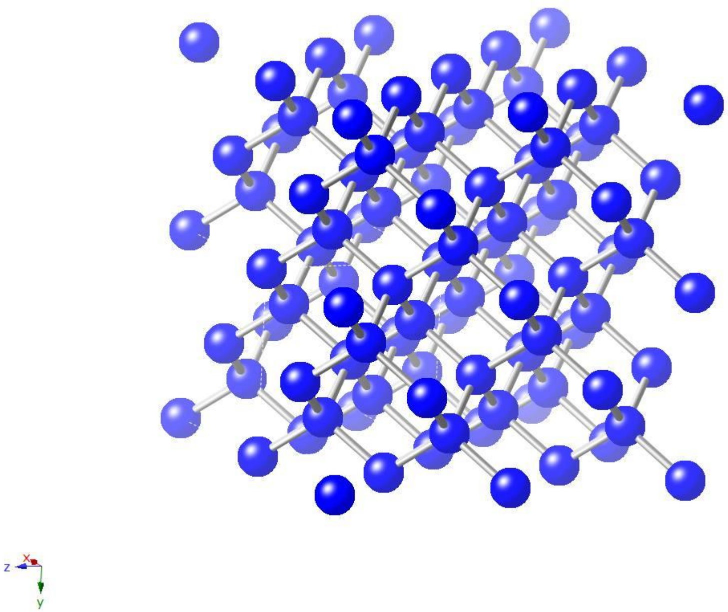

- Si(111)

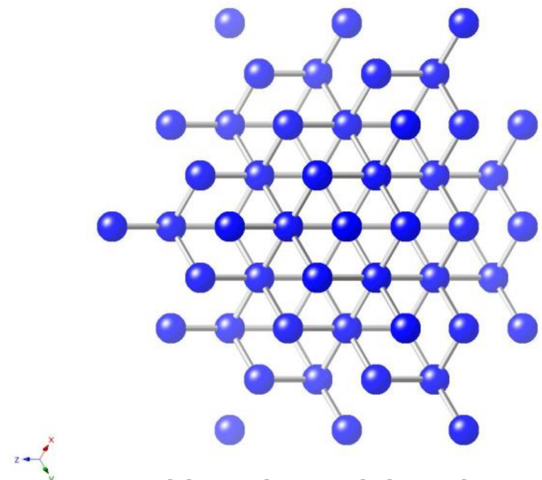

- Si(111) – side view

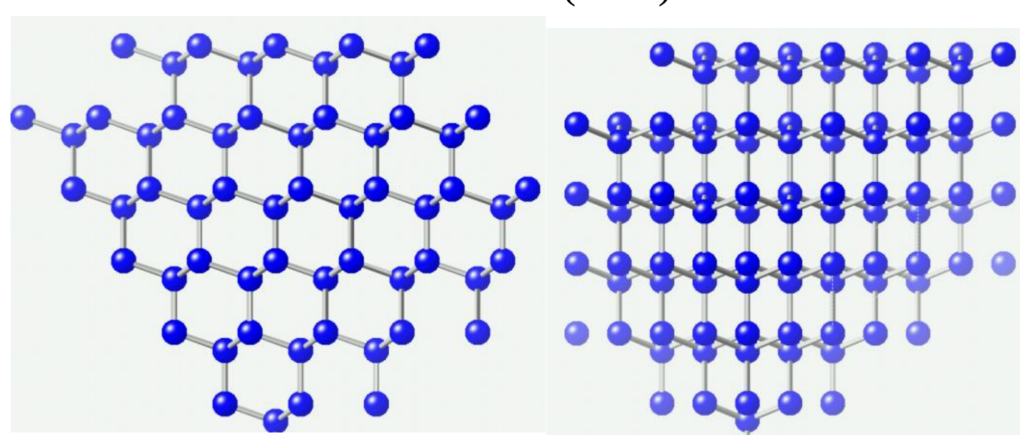

Use crystal structure of the substrate

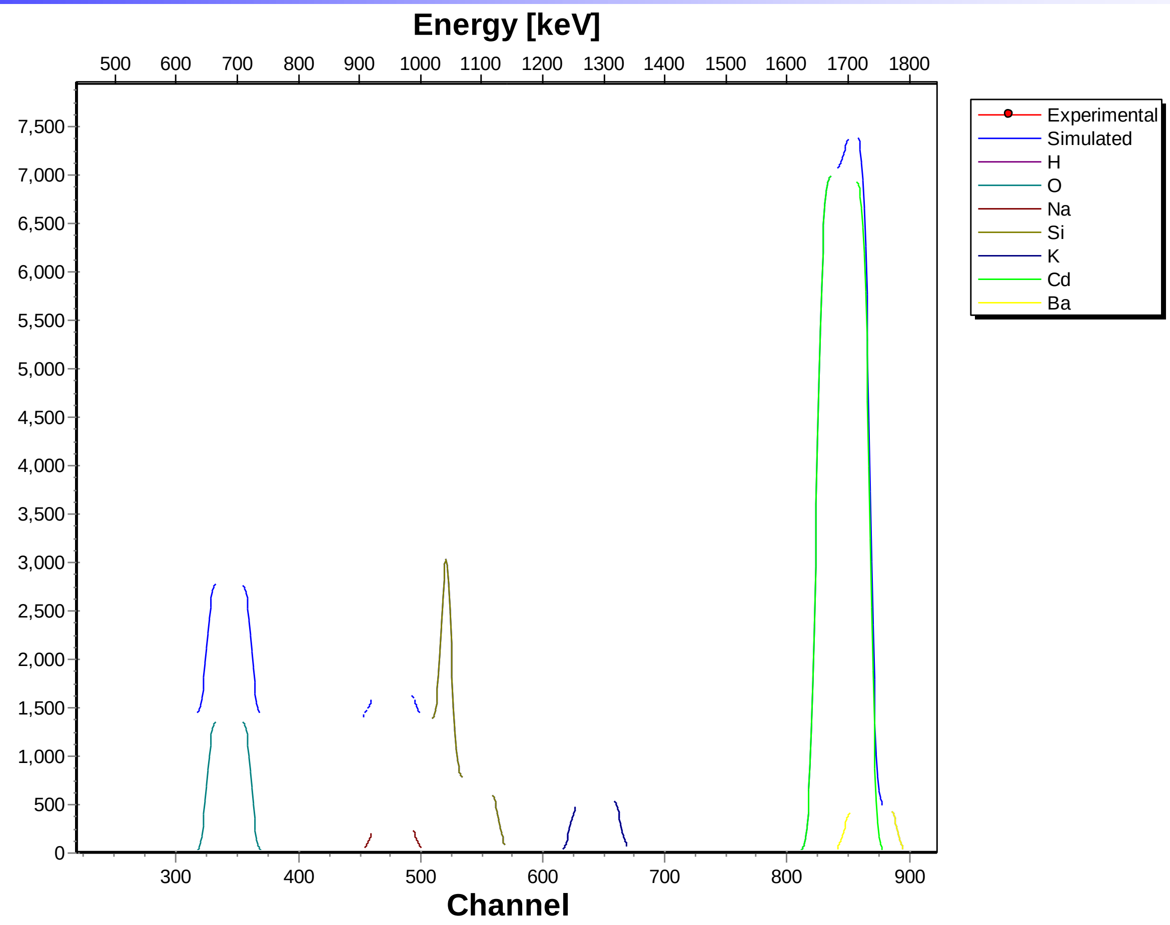

- Substrate can be aligned to a major crystallographic direction to minimize background signal in some cases

Elastic Recoil Detection (ERD)

Heavy Elements by MEIS or RBS

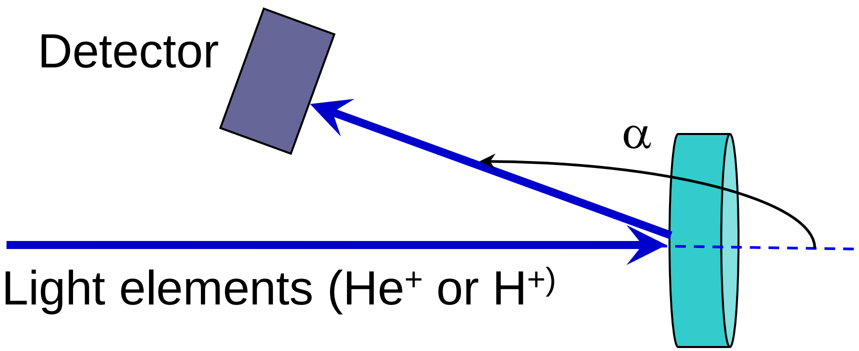

Light Elements by Elastic Recoil Detection

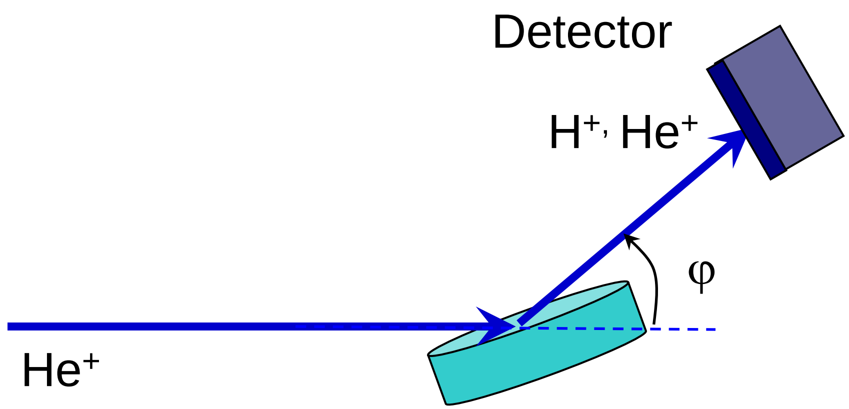

~150nm SiONH/Si(001)

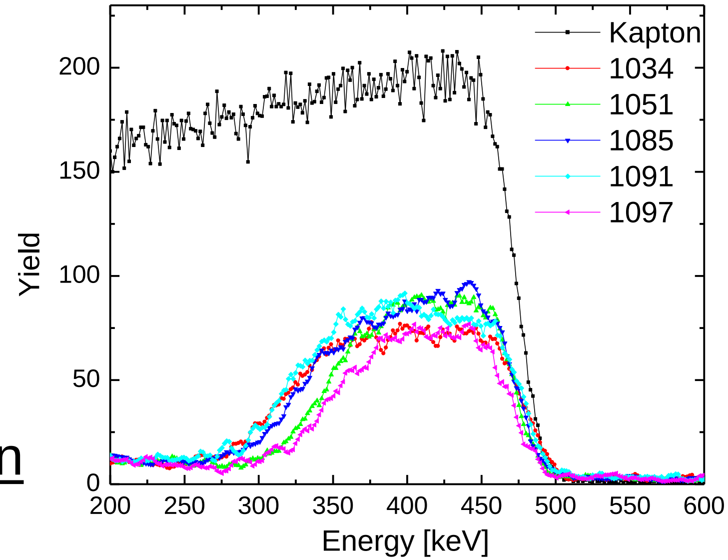

"Classical" ERD

Incident energy = 1.6MeV He^+

Incident angle = 75°

Recoil Angle = 30°

Al-mylar (range foil)

ERD Principles and Limitations

$$E_2 = k\,E_0$$

$$k = \frac{4M_1 M_2}{(M_1 + M_2)^2}\cos^2\phi$$

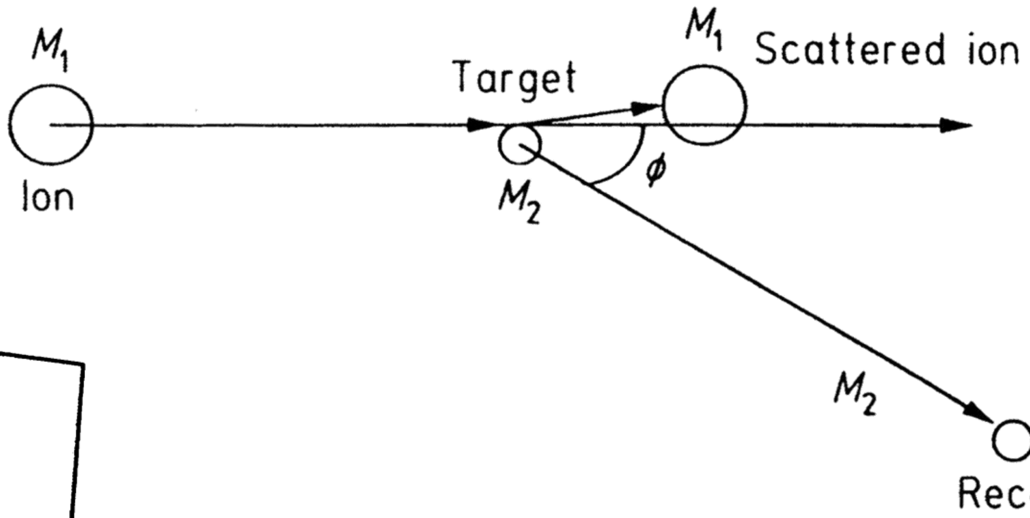

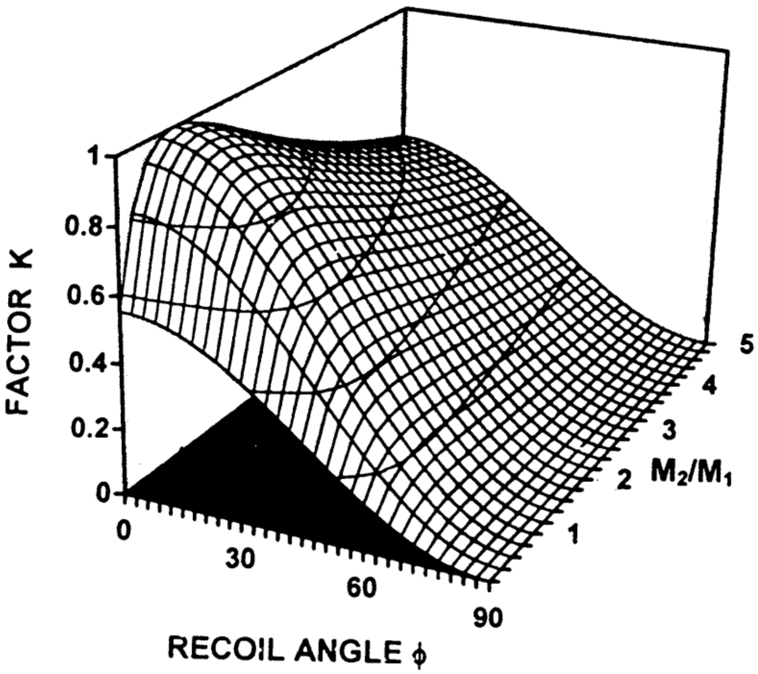

<u>Some advantages of ERD</u>:

good dynamic range;

excellent hydrogen sensitivity;

very well suited for analysis of light elements

<u>Some disadvantages</u>:

Resolution (limited by detector, ~10-15keV);

sensitivity to surface contamination

RBS plus ERD ⇒ Full Stoichiometry!!!

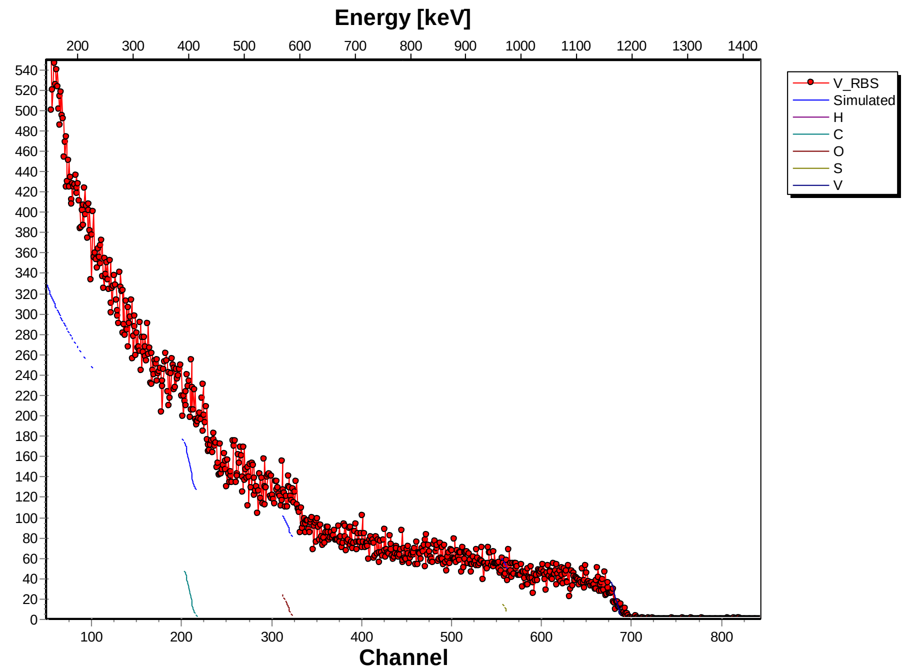

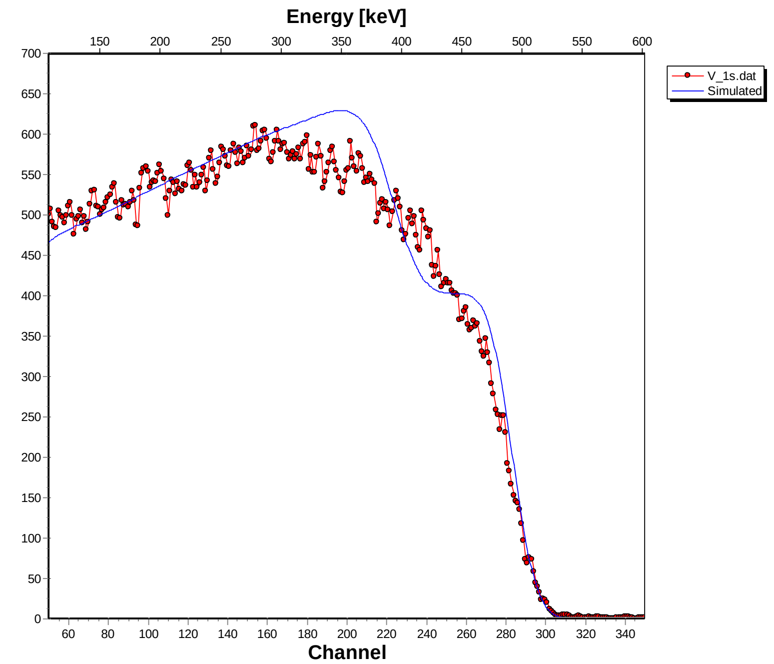

RBS and ERD results for $\mathbf{VS_xO_yC_z{:}H}$

Assumption: ~ 900Å $V_{0.03}S_{0.03}O_{0.25}C_{0,44}H_{0.25}$/(bulk) $V_{0.03}S_{0.03}O_{0.13}C_{0,44}H_{0.37}$

A comparison between RBS and MEIS

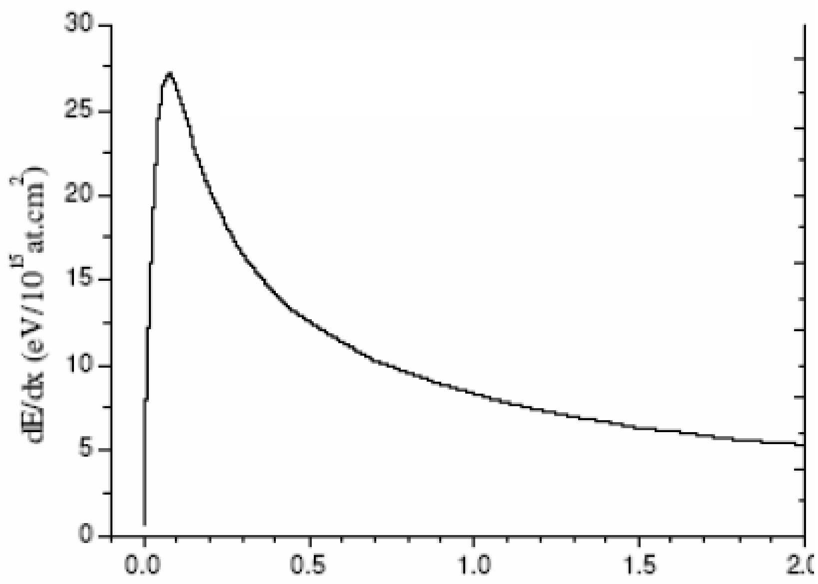

Close to maximum of ~ 14 eV/Å at ~ 100 keV!
This helps, but the greater advantage is the use of better ion detection equipment!

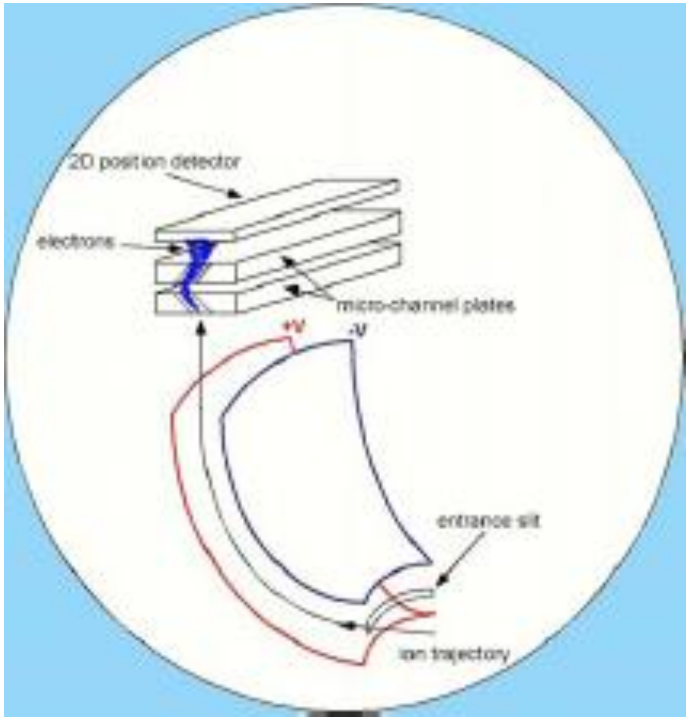

	RBS	MEIS
Ion energy	~ 2 MeV	~ 100 keV
Detector resolution	~ 15 keV	~0.15 keV
Depth resolution	~ 100 Å	~ 3 Å

2 basic advantages vs. RBS: Often better dE/dx, superior detection equipment

Medium Energy Ion Scattering (MEIS)

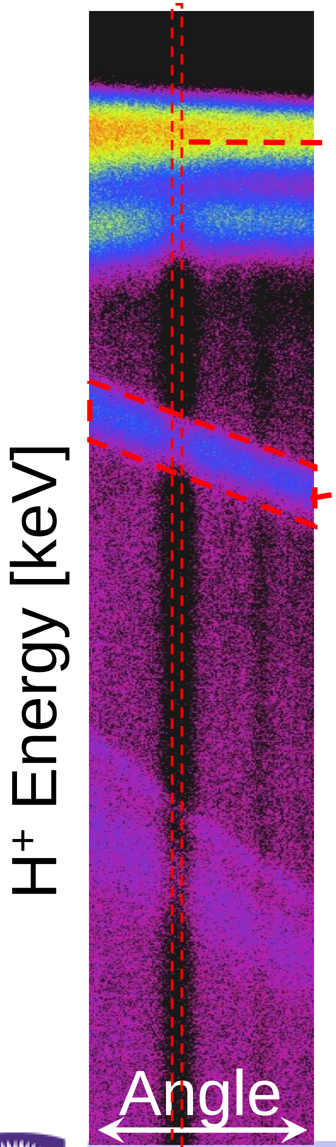

Energy distribution for ***one*** *angle*

Angular distribution for ***one*** *element*

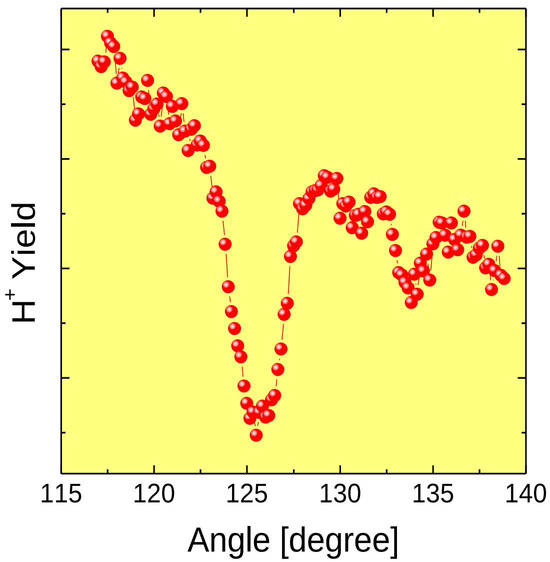

100keV H^+, SiO_2/poly-Si/ZrO_2/Ge(100)

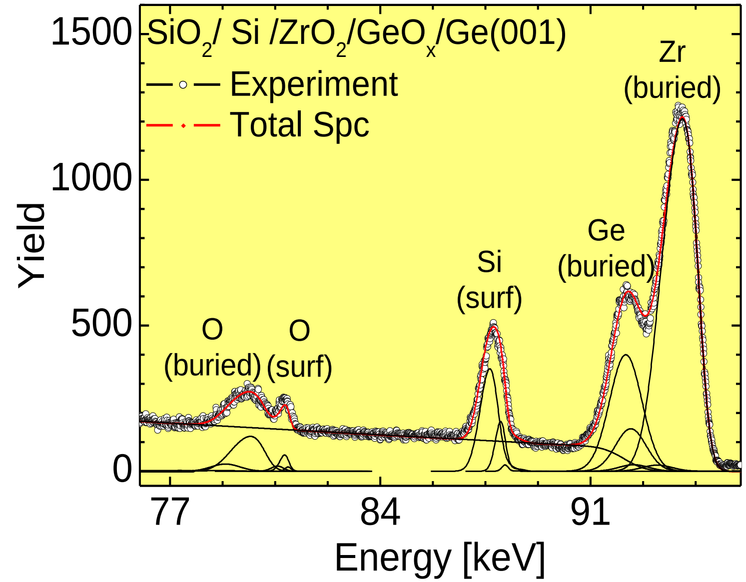

Energy distributions:

- mass (isotope) specific
- quantitative (2% accuracy for high-Z)
- depth sensitive (at the sub-nm scale)

Western

MEIS analysis of as-deposited films

98keV H^+
Sample Alignment:
Si(001) incident; Si(110) outgoing

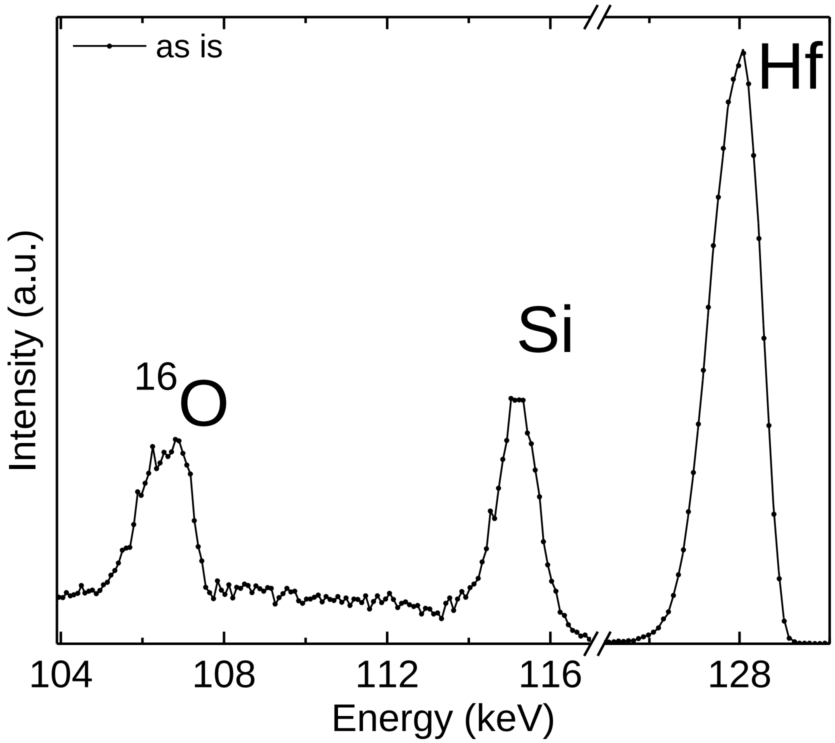

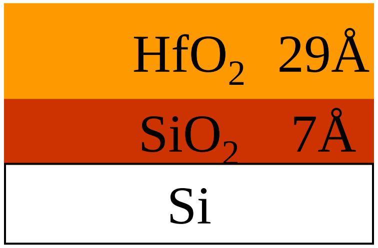

TEM:
2.8nm HfO_2/1nm SiO_2/Si(001)

Depth resolution and concentration profiling

Basic concept: Depth profile is based on the energy loss of the ions traveling through the film (stopping power $\varepsilon \propto dE/dx$).

Example: Depth resolution for ≈95 keV protons
With MEIS spectrometer ≈180 eV *vs* RBS detector ≈15keV

- Stopping power $SiO_2 \approx 12$ eV/Å; $Si_3N_4 \approx 20$ eV/Å;

Layer model:

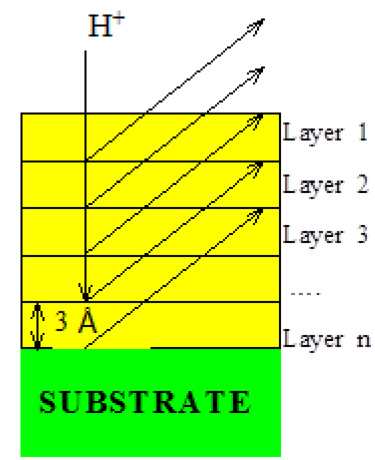

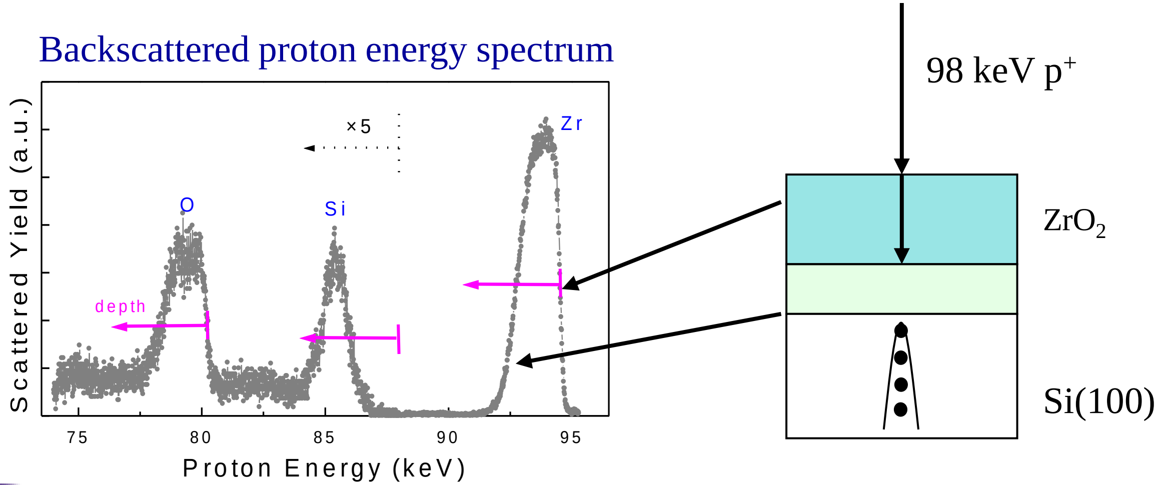

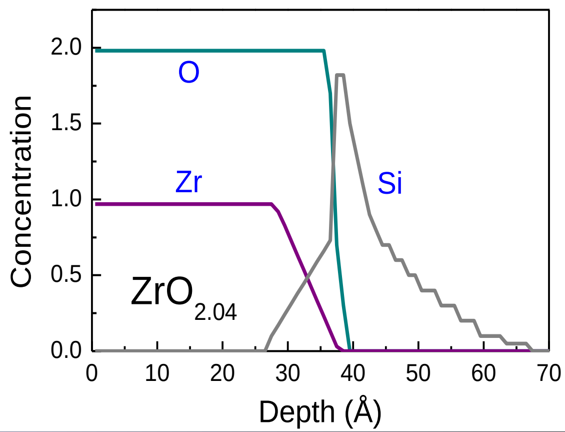

Western

Oxidation temperature dependence: ^{16}O and ^{18}O

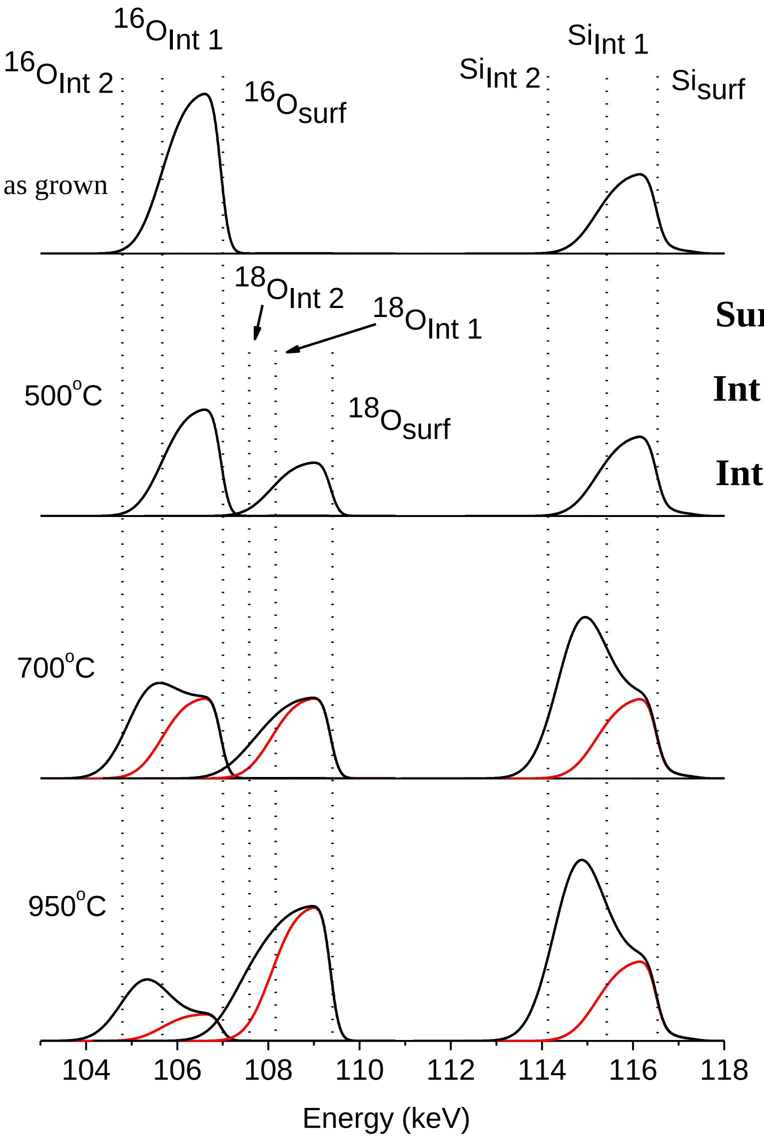

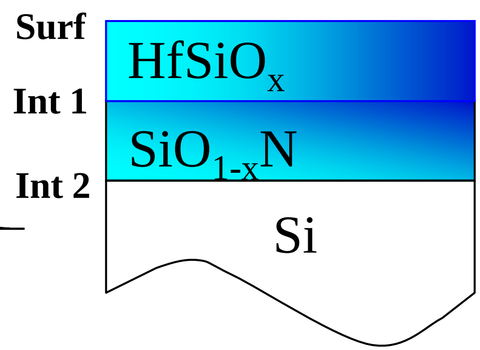

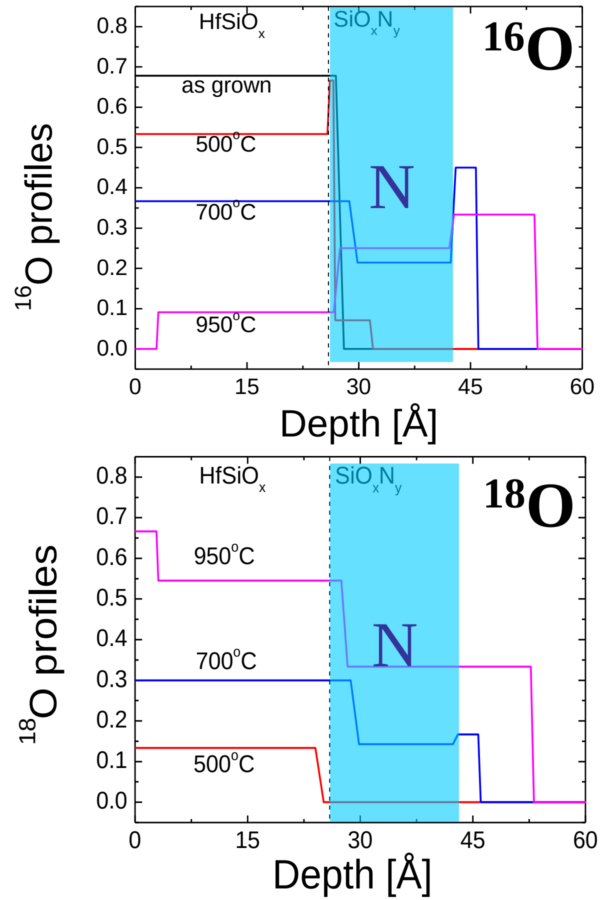

O reaction with Si → deeper than N distribution

Oxygen diffusion in oxides

Oxygen (O_2) transport in **SiO_2**

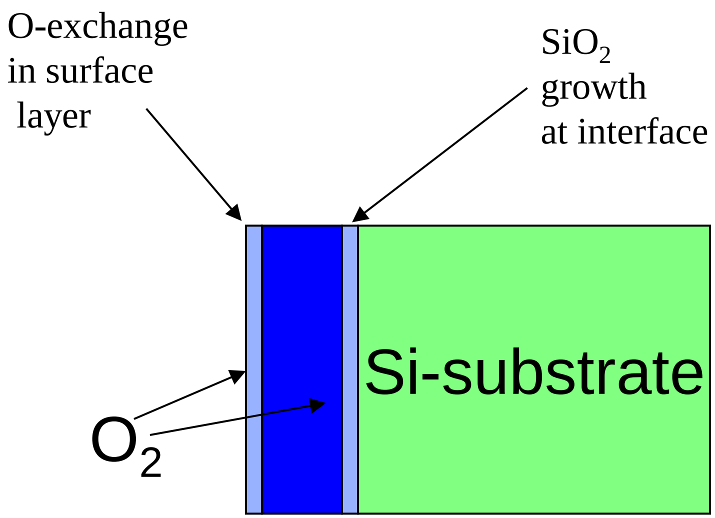

Atomic oxygen (O) transport in **metal oxide films**

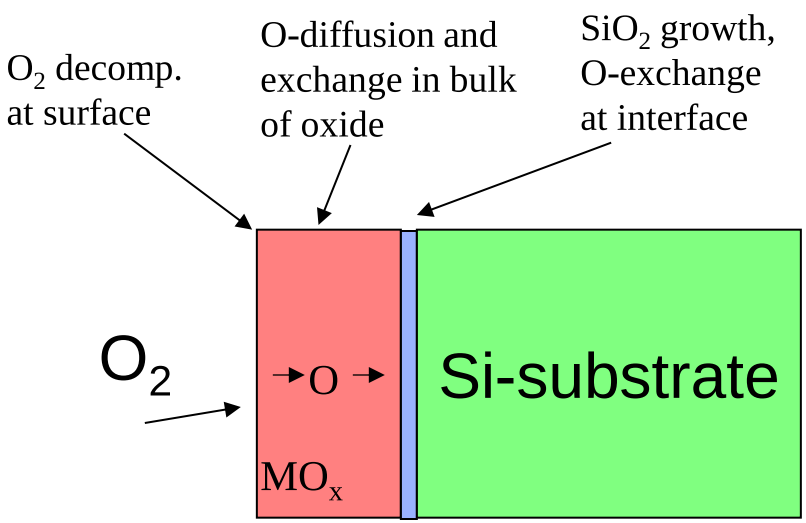

SiO_2 films:

- **amorphous** after annealing
- molecular O_2 transport in SiO_2
- decomposition by SiO desorption

(Many) **metal oxide** films:

- tend to crystallize at **low T**
- atomic O transport in the film
- high oxygen mobility

Western

Diffusion and interface growth in HfO_2 and $HfSiO_x$ ultrathin films on Si(001)

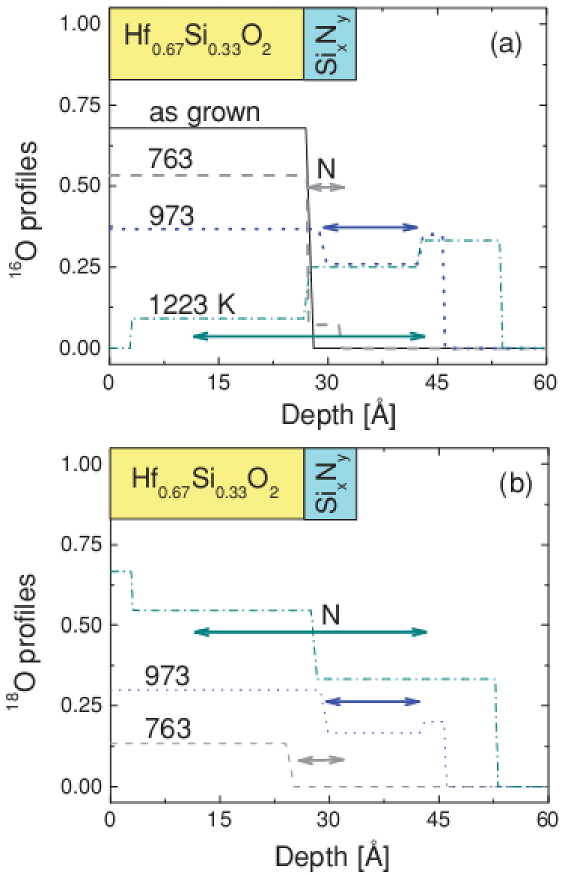

	T (°C)	Time (min)	Oxide growth (Å)
High-k	700	30	11
	800	30	18
	950	30	25
SiO_2*	750	165	5
		2640	10
	900	60	10
		1860	27

- **Faster interfacial SiO_2 growth in case of high-κ oxides in comparison to the SiO_2 thickness growth for bare Si**

L.V. Goncharova, M. Dalponte, T. Feng, et al, *PRB* **83** (2011) 115329

Western

***Gusev, Lu, Gustafsson, Garfunkel, *PRB* 52 (1995) 1759.**

Part II: Ion Implantation

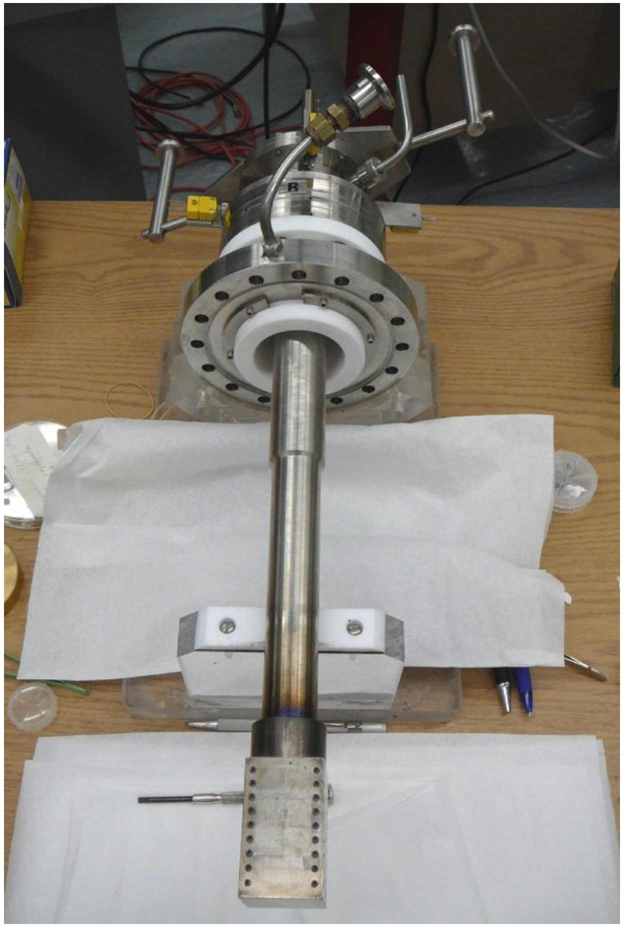

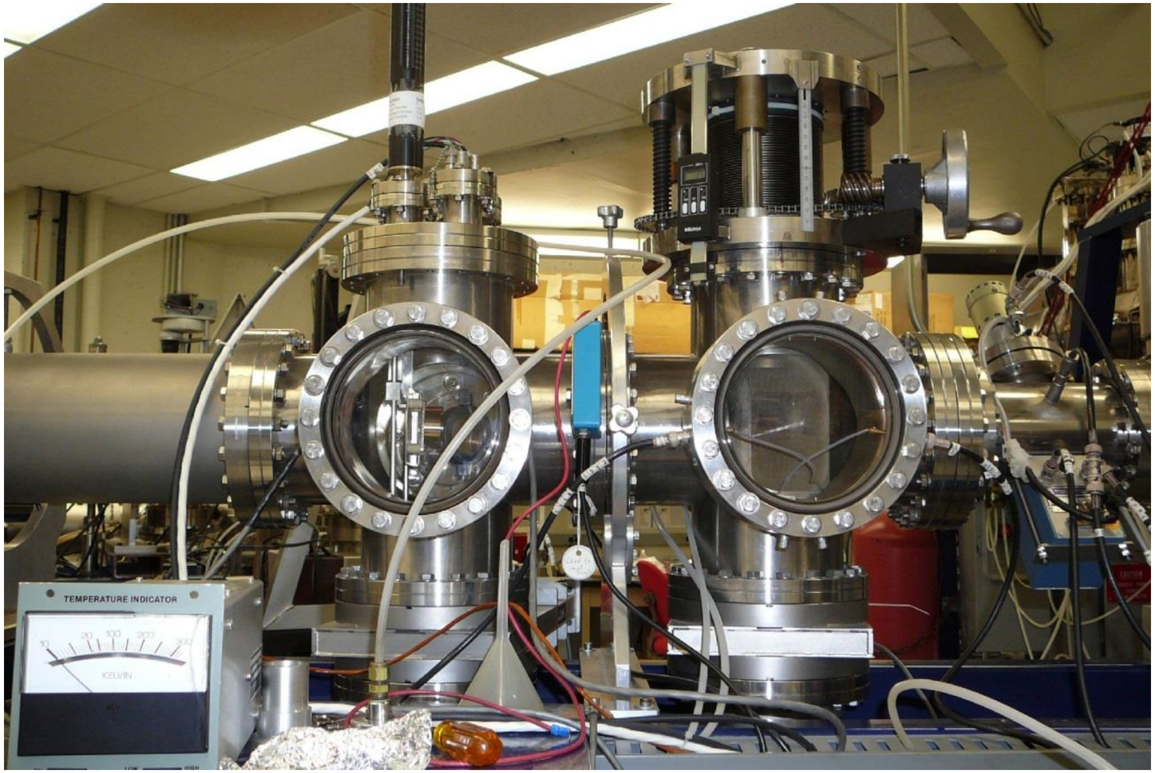

- Implantation chamber and implantation stage

Periodic Table

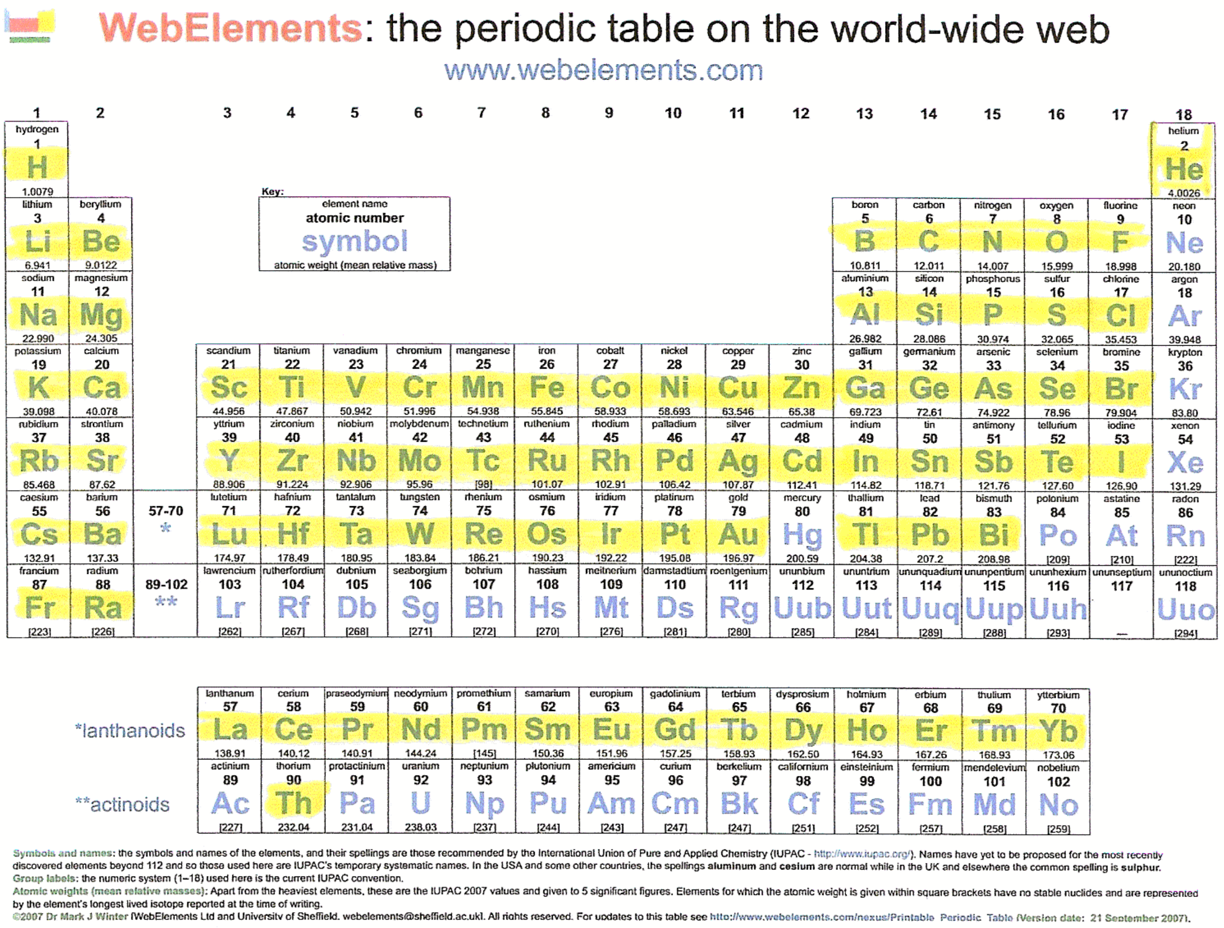

- ***We can produce beams of all those elements shown in yellow !***

Ion Implantation

aperture

(e.g.
area = A = 1.13 cm^2)

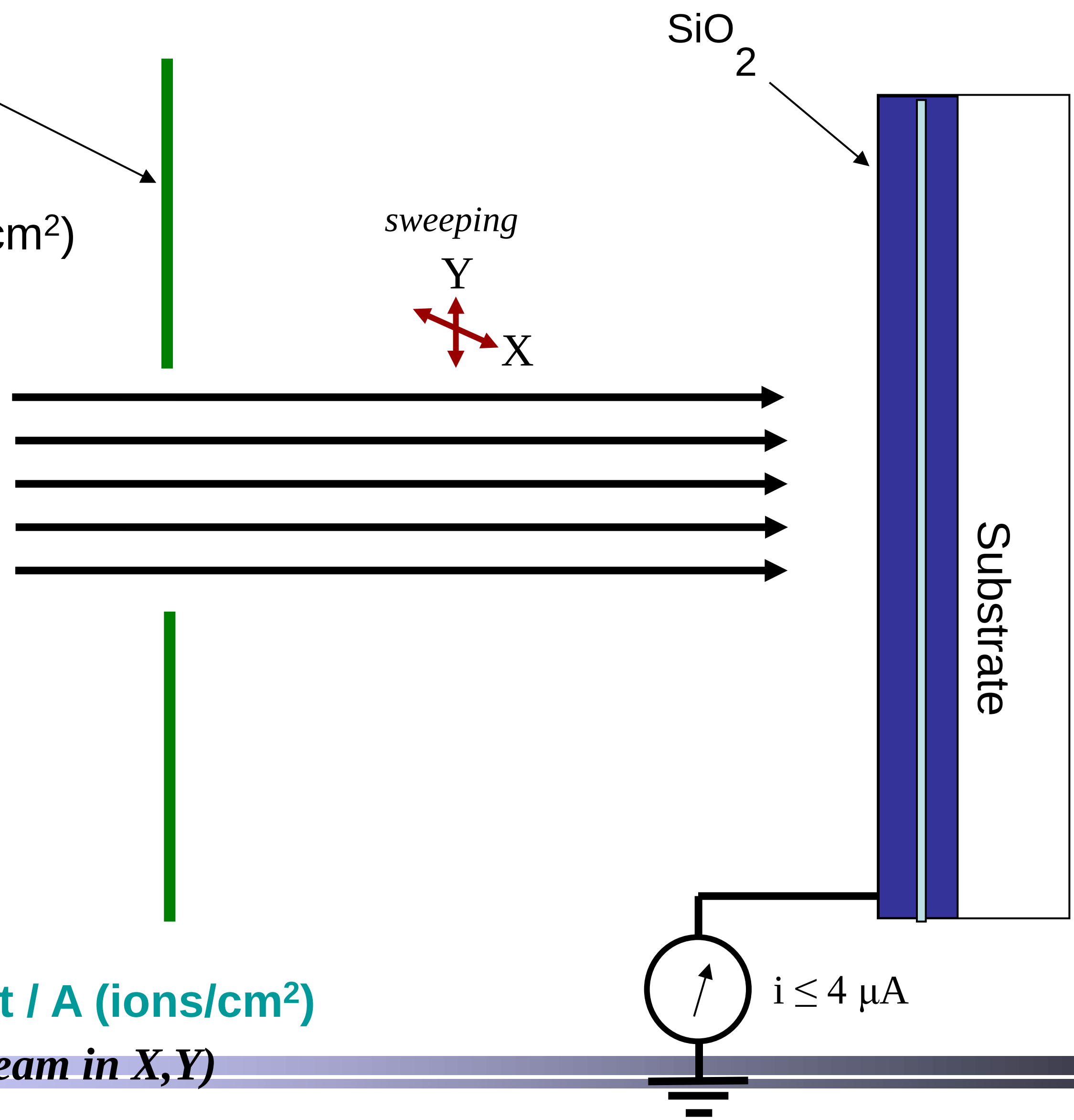

Si^- ions

(from
Tandetron)

(@ 25-2,000keV)

Dose = i Δt / A (ions/cm^2)

(raster beam in X,Y)

Stopping and Range of Ions in Matter (SRIM)

http://www.srim.org/ ⇒Download SRIM-2008

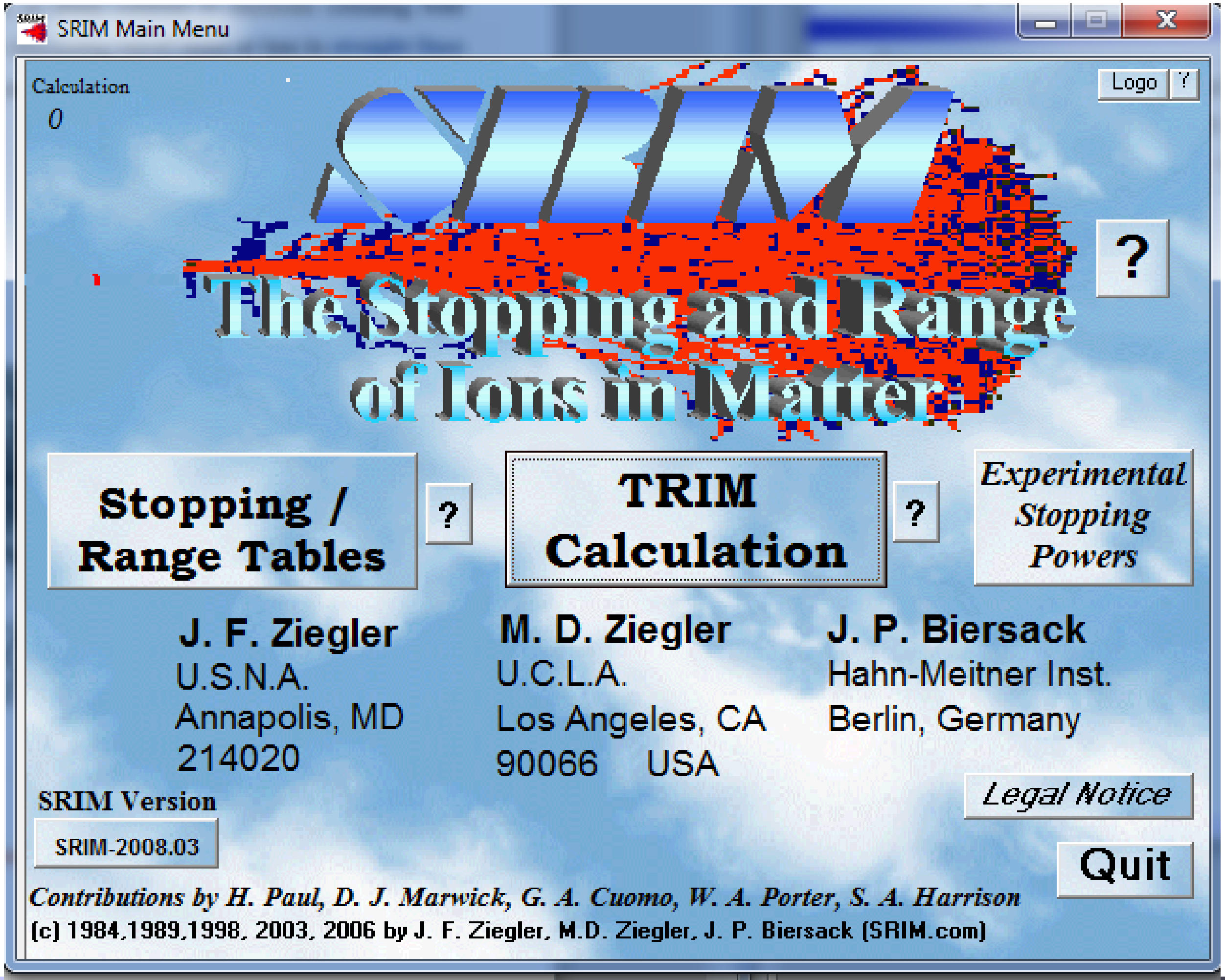

SRIM Setup Window

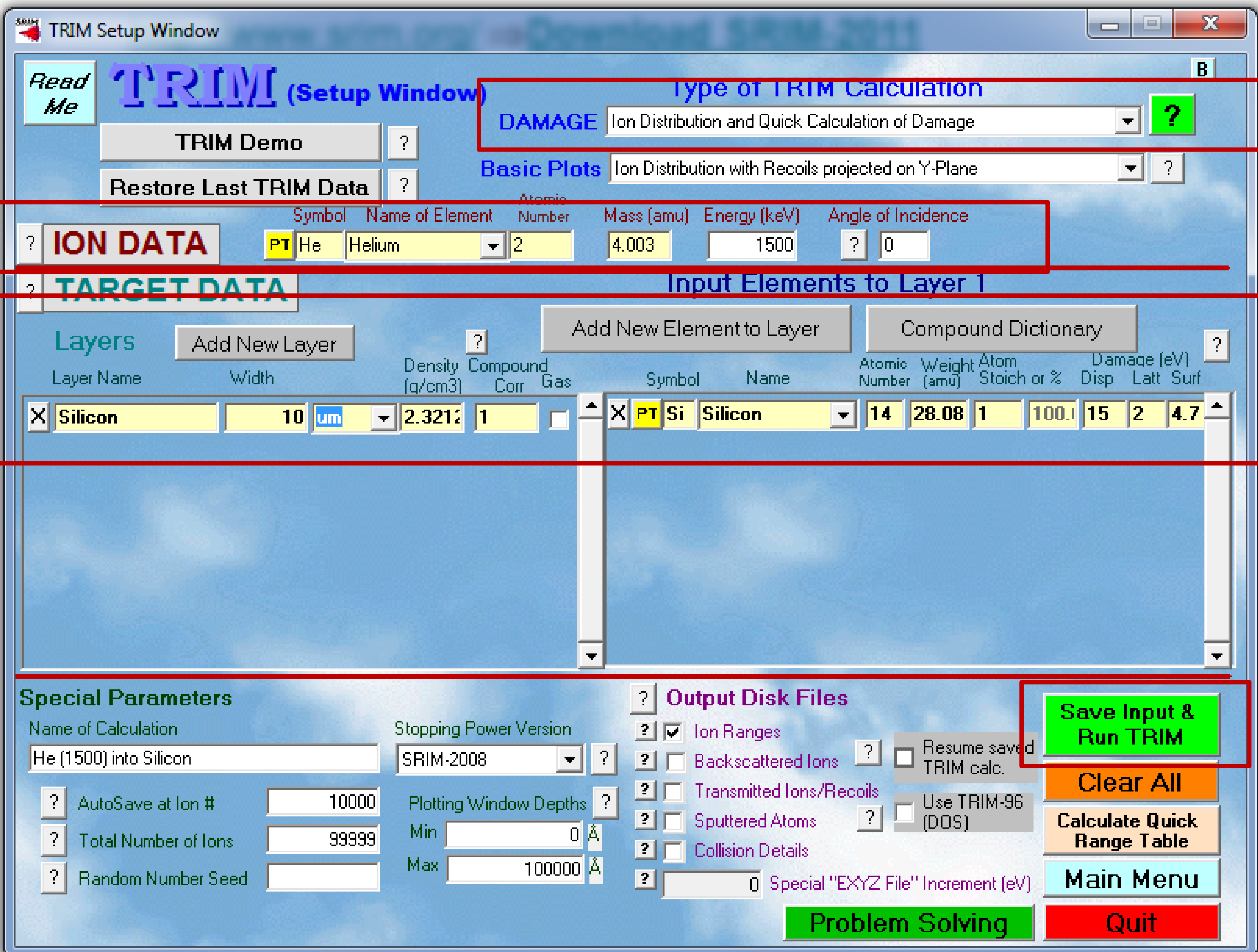

Calculated Ion Trajectories

2MeV He^+ in Si | 50keV He^+ in Si | 50keV Au^+ in Si

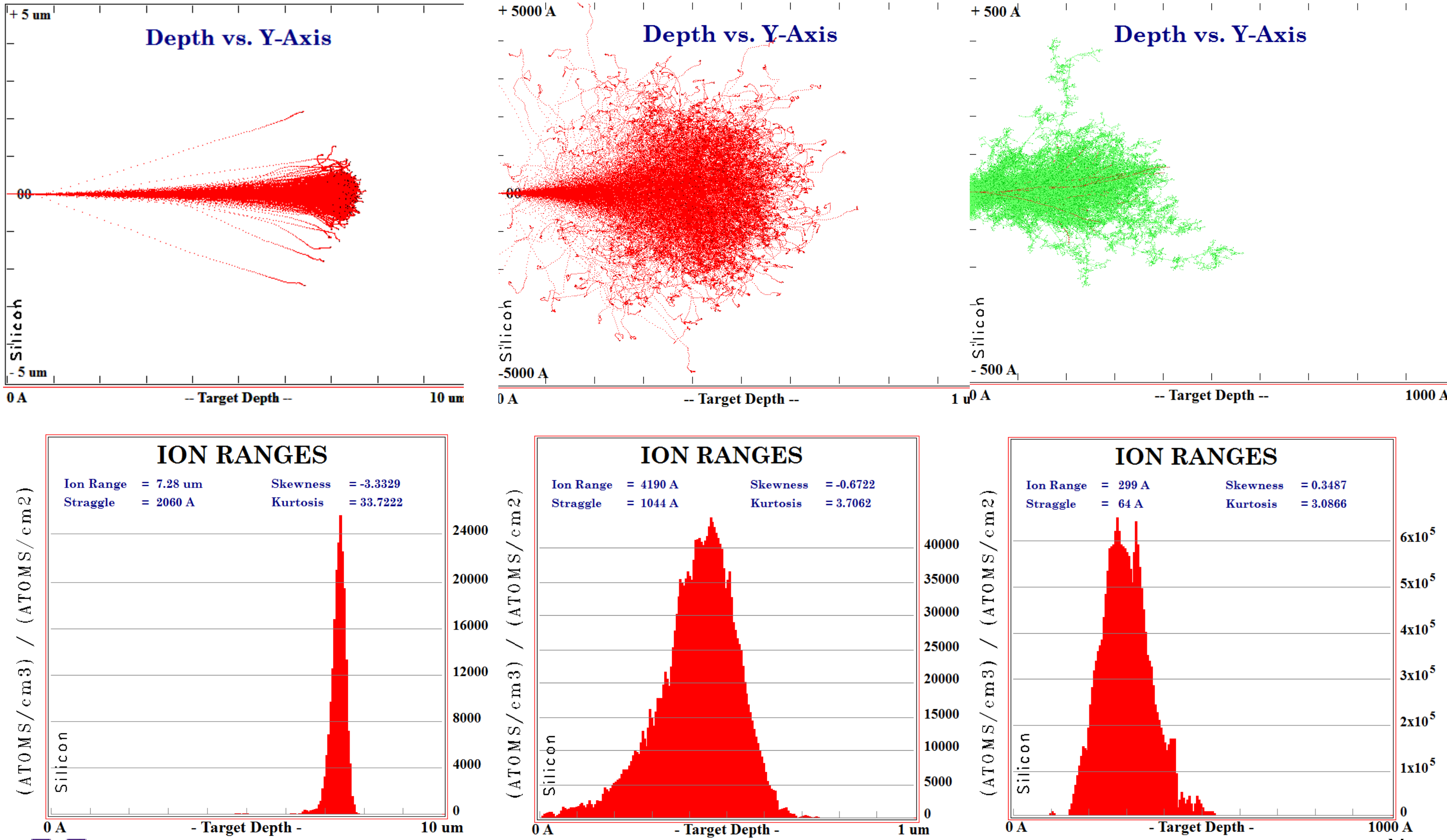

Ion-implanted Si and Ge quantum dots in dielectrics

- Second generation Si and Ge photonics
- Strong light emission from nanocrystals or quantum dots (QD) by reducing the size of Si to < a_{Bohr} (Si ~3-5nm; Ge ~ 24nm)
- Porous Si and crystalline QW
- Bonafos et al. used TEM to relate Si QD to excess Si (10, 20, 30%)

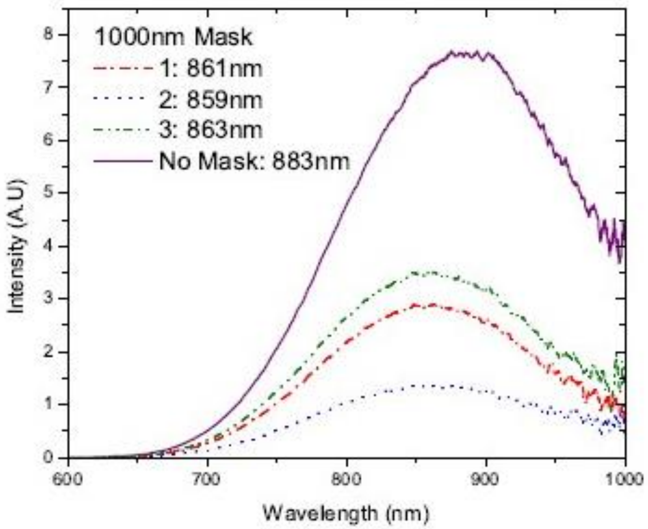

Barbagiovanni et al, MRS (2009)

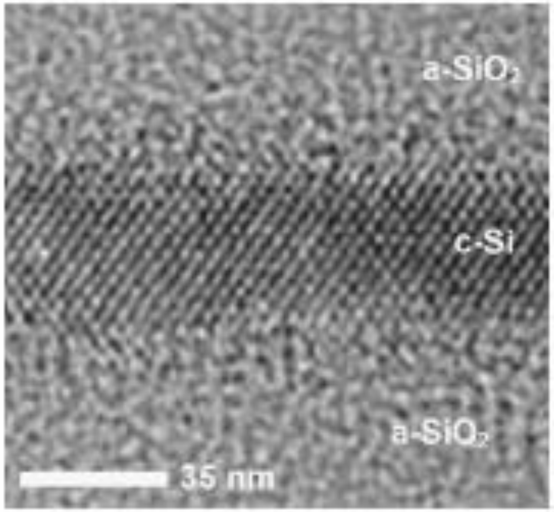

Cho et al, JAP 2007

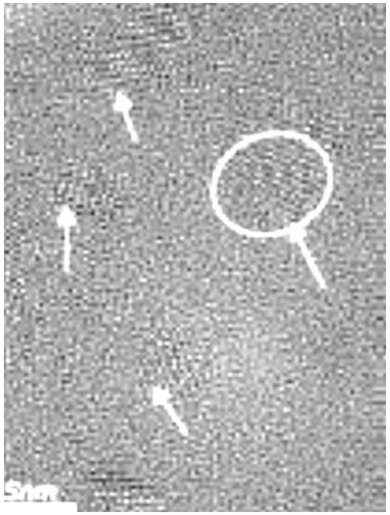

Bonafos et al, NIMB (2001)

Growth of Si-QD

- RT Implantation Si^- (Ge^+) 90keV $5x10^{16}$ -$1x10^{17}$ions/cm^2
- 120min @1100^0C (Si) or 900^0C (Ge) in furnace,
- 60 min @500^0C in N_2/H_2 gas

- Early stage of formation governed by diffusion

$$\frac{\partial C_{Si}}{\partial t} = -4\pi rND\ (C_{Si} - C_{sol})$$

- Eventually Ostwald ripening

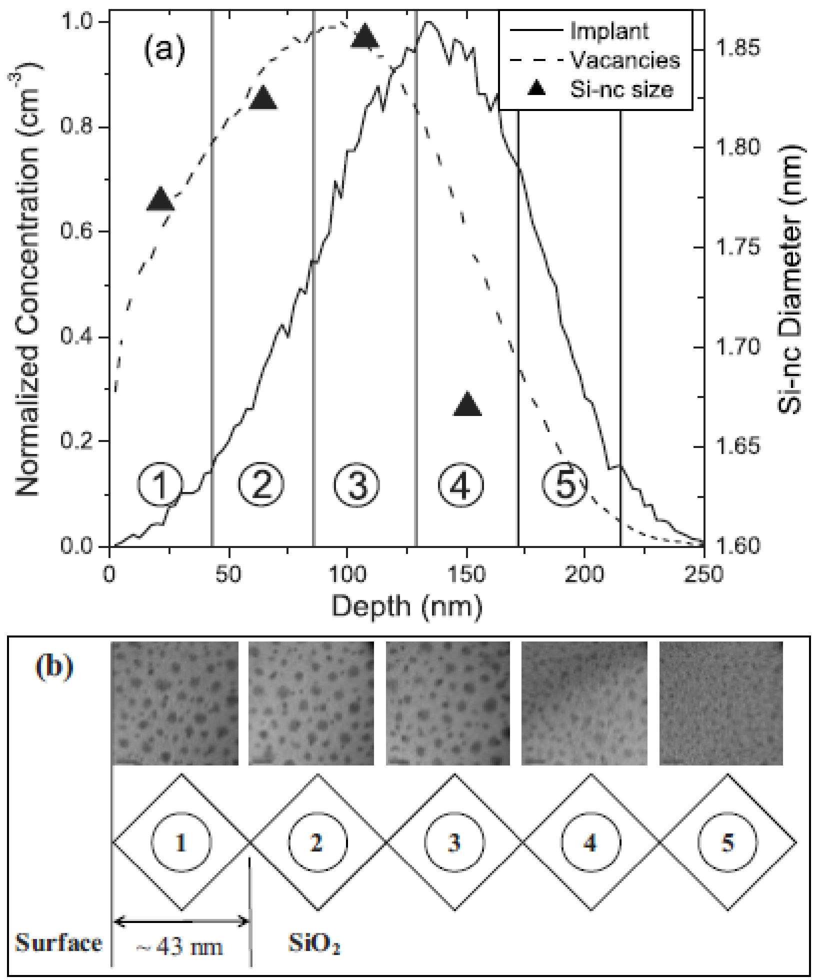

Link between defects in the SiO_2 and formation of Si-QDs

Mokry C.R., Simpson P.J., Knights A.P. *J. Appl. Phys*. **105** (2009) 114301

Ge in Al_2O_3(0001): crystallization and ordering

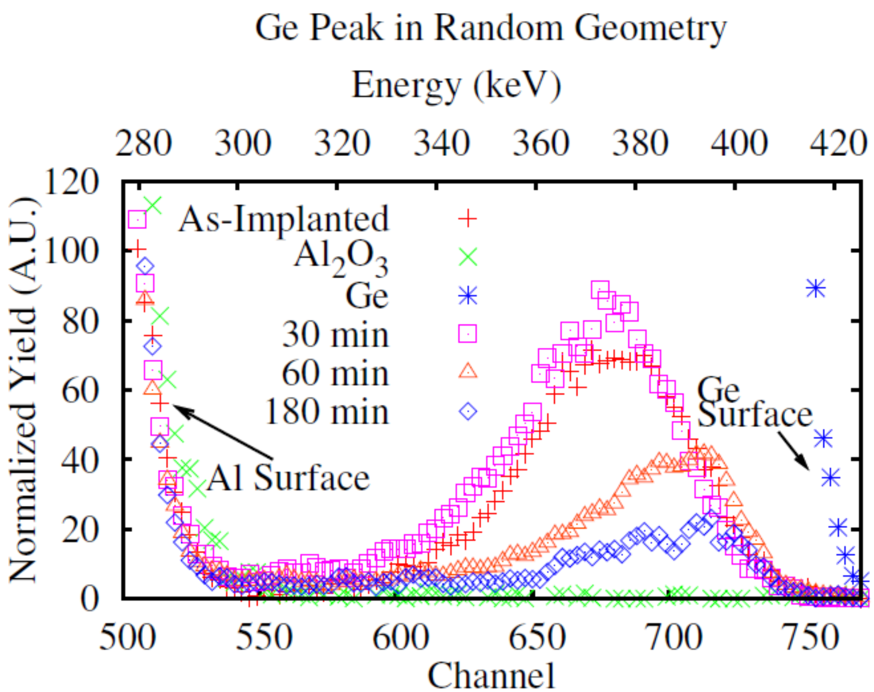

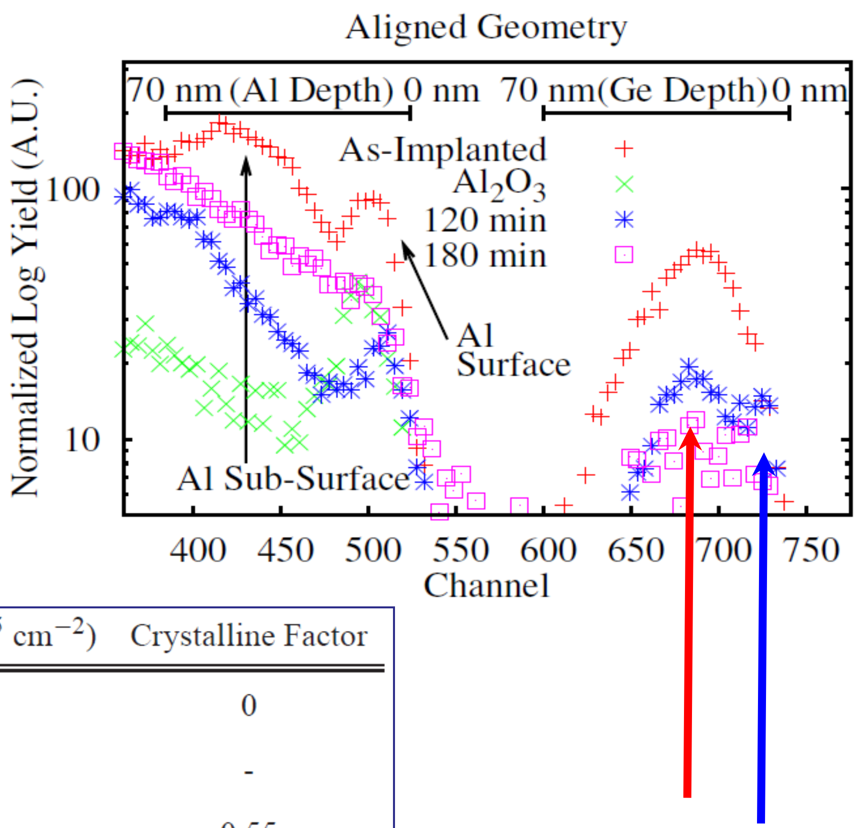

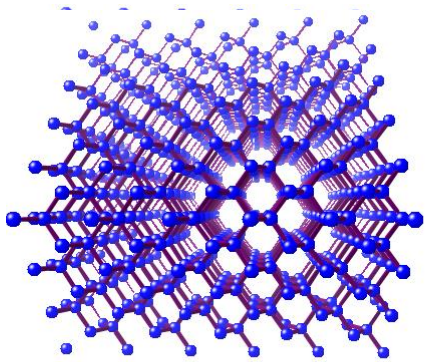

Sample (min)	Concentration ($\times 10^{15}$ cm^{-2})	Crystalline Factor
As-Implanted	9.87	0
30	6.68	-
60	3.35	0.55
120	4.17	0.55
180	1.63	0.5

E.G. Barbagiovanni, S.N. Dedyulin, P.J. Simpson, L.V. Goncharova, *NIMB* **272** (2012) 74–77

XPS

Sample (min)	Concentration ($\times 10^{15}$ cm^{-2})	Crystalline Factor
As-Implanted	9.87	0
30	6.68	-
60	3.35	0.55
120	4.17	0.55
180	1.63	0.5

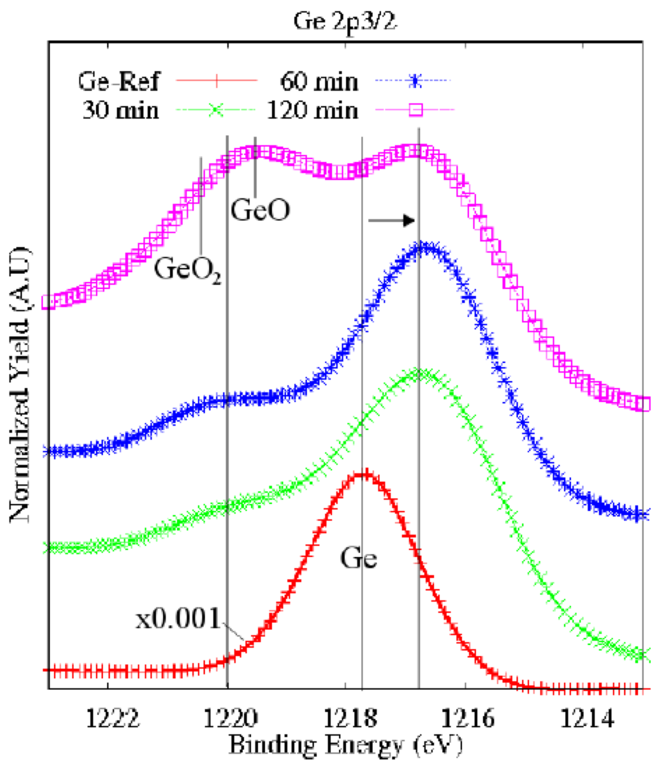

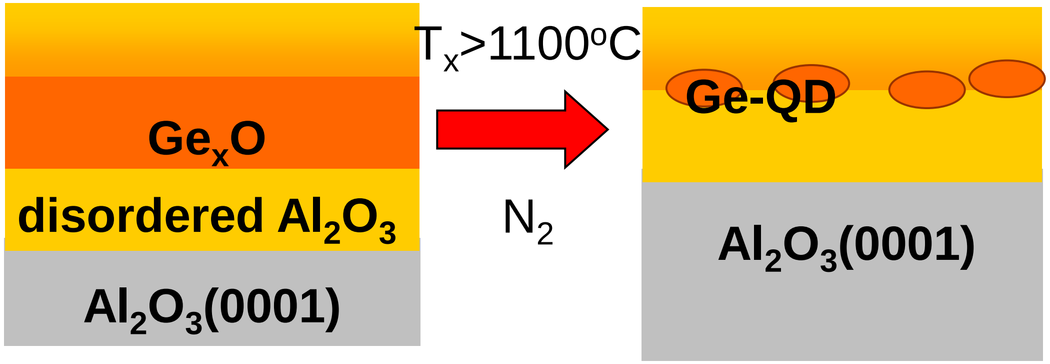

Ar sputtering prior to XPS analysis:
Ge layer is 3-5nm deep

- Shift of Ge peak towards the surface (RBS)
- GeO_x peaks in XPS $\Rightarrow$ Ge loss via GeO desorption

Western

Cross-sectional TEM micrographs

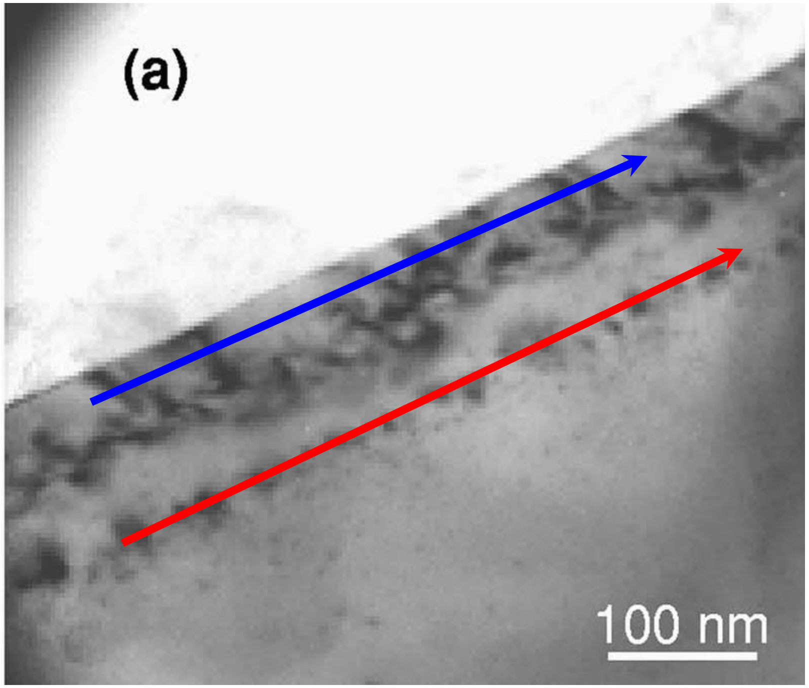

- Contrast arising from stress fields and end of range implantation damage

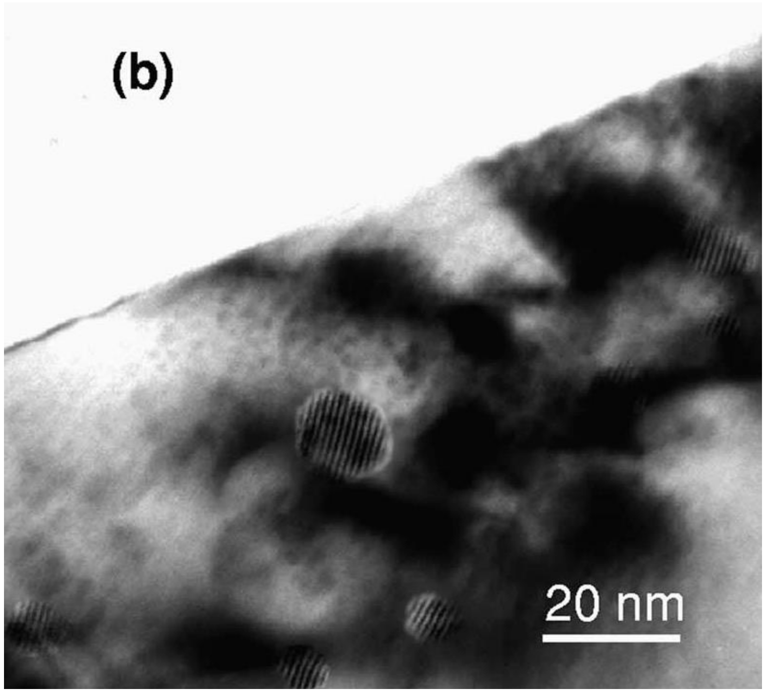

- Moiré fringes become visible from the overlap of the crystal planes of Ge QD and the sapphire matrix

Ge in $Al_2O_3(0001)$: crystallization and ordering

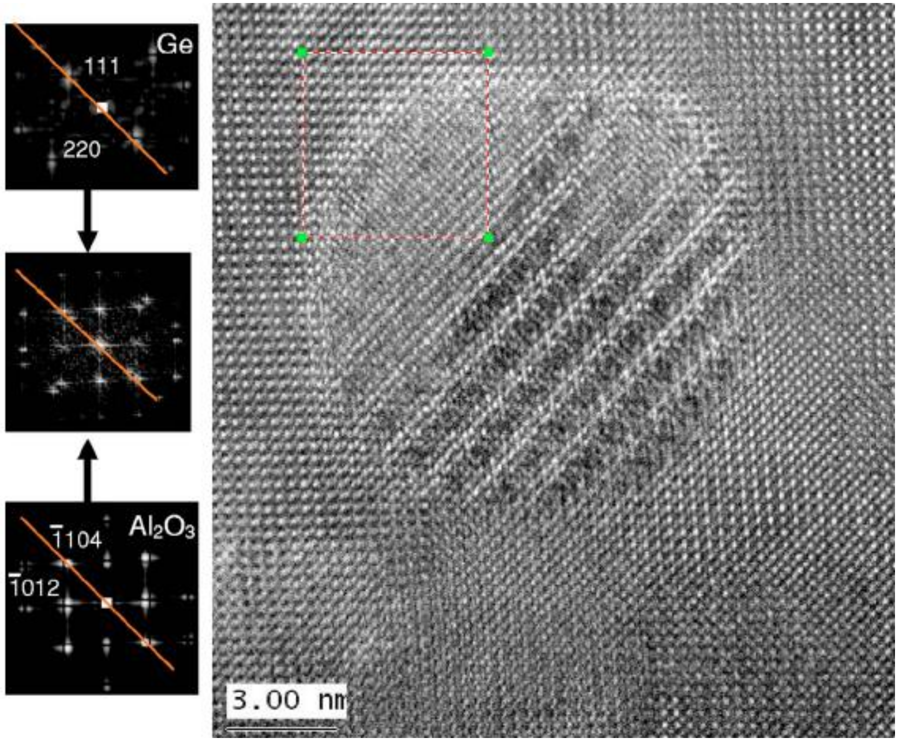

- Slow diffusion rate of the alumina matrix atoms at < T_{melt}
- Ge blocking minimum can be related to the stereographic projection of the sapphire crystal and corresponds to the [111] scattering plane:

$$(1\underline{1}04)\ Al_2O_3\ //\ (111)Ge \quad \text{and} \quad [\underline{2}11]\ Al_2O_3\ //\ [\underline{11}2]\ Ge$$

I.D. Sharp, Q. Xu, D.O.Yu, et al. *JAP* **100** (2006) 114317

Conclusions and future directions:

- Ion Beam Analysis is an enabling technology for thin film scientists and engineers
- Our goals are to initiate collaborative research projects and stimulate multidisciplinary interactions, To enable the use of ion beams, including the introduction of ion beam methods to new discipline areas
- Development of novel ion beam analyses techniques

References:

1) L.C. Feldman, J.W. Mayer (1986) Fundamentals of Surface and Thin Film Analysis.
2) Y. Wang, M. Nastasi (2010, or previous edition) Handbook of Modern Ion Beam Materials Analysis.
3) The Stopping and Range of Ions in Matter (SRIM), http://www.srim.org/

Elastic recoil detection for negative ions

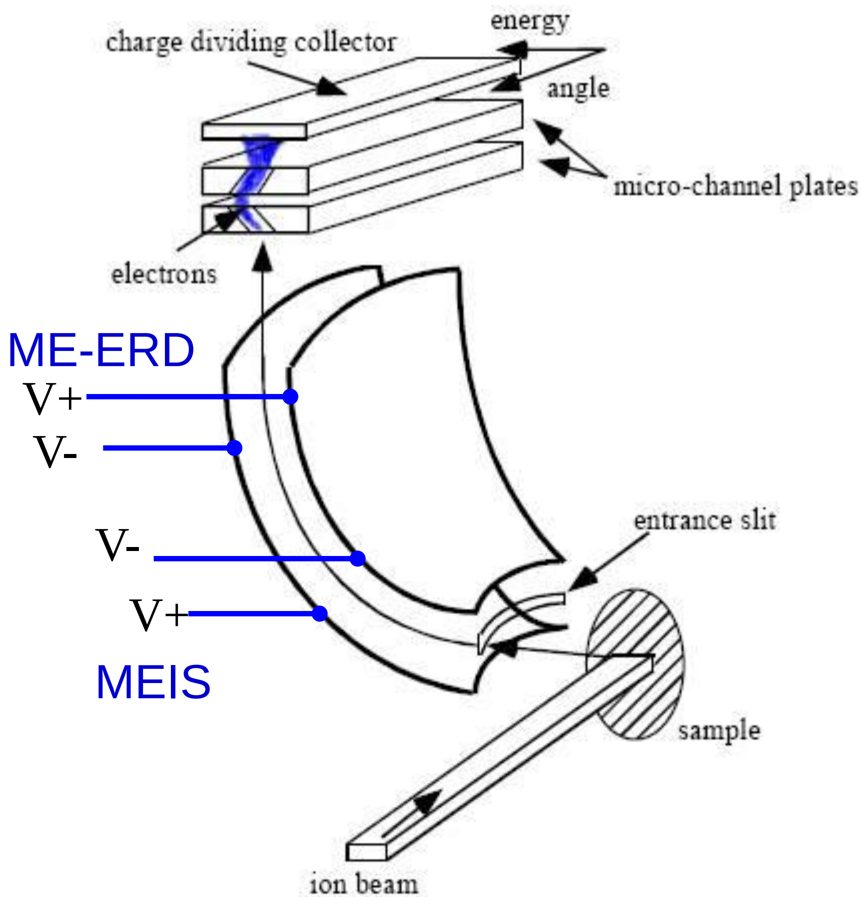

Toroidal Ion Energy Analyzer (HVEng, Amersfoort, The Netherlands)

Crucial points for detecting H ion recoils directly are:

- To increase the recoil cross-section
- To reduce (to suppress) the background originating mainly from elastically scattered incident ions

Only charged particles are detected by TEA

⇒ use incident beam ions without negative ion fractions and detect negative H^- recoils

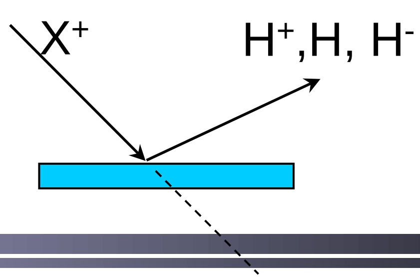

Control QD Distribution with Mask

Si QD nucleation and growth by Si ion implantation and anneal ⇒

Lateral separation between implanted regions

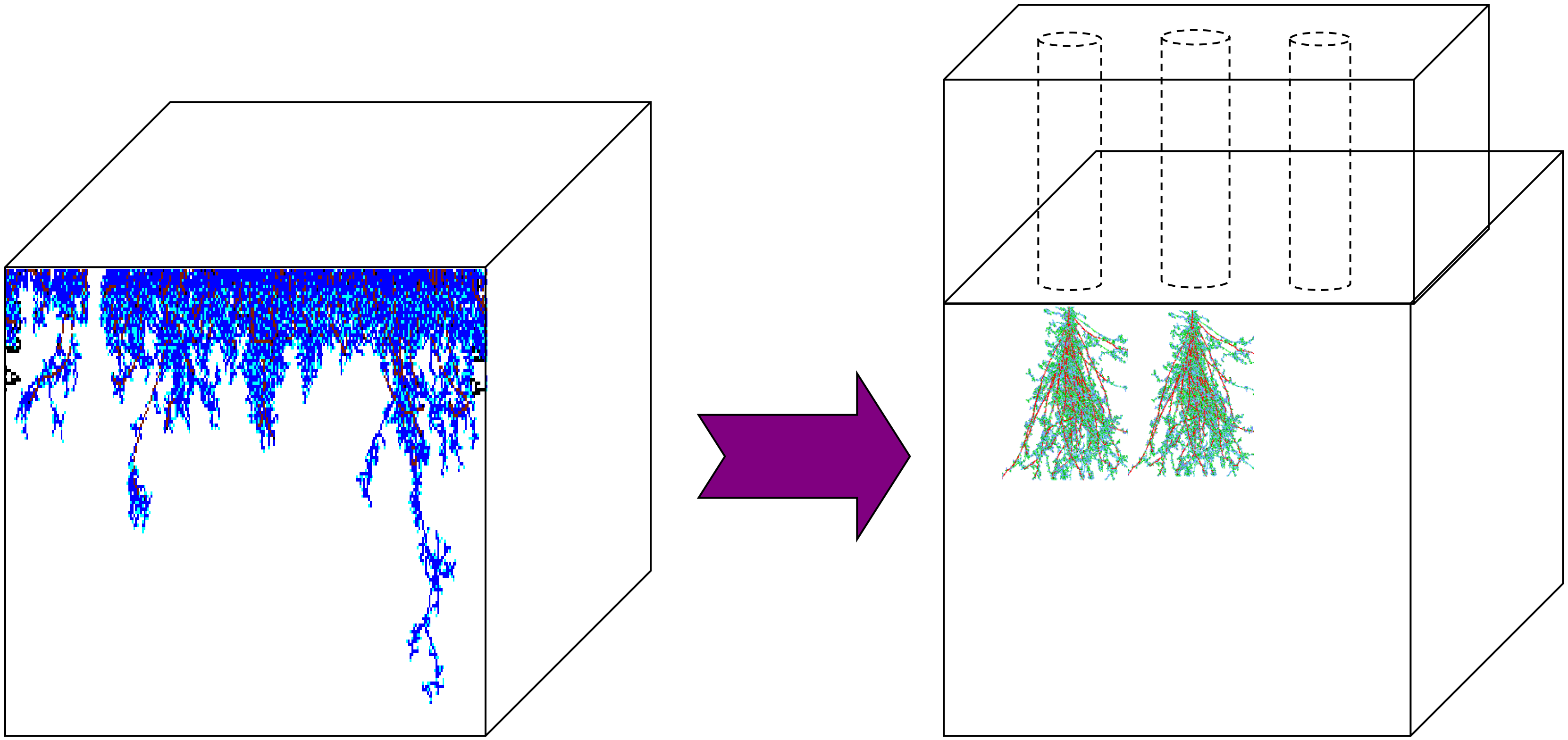

Thank you!

Lyudmila V. Goncharova

Department of Physics and Astronomy,

Western University, London, Ontario

lgonchar@uwo.ca